Thermodynamic Analysis of Solar Based Polygeneration Systems for a Residential Community

A thesis submitted in partial fulfilment of the requirement for the degree of

Doctor of Philosophy

In

Mechanical Engineering

by

FAIZAN KHALID

(Roll No--2K19/PhD/ME/19)

Under Supervision of

Prof. Rajesh Kumar

Department of Mechanical Engineering
Delhi Technological University

Department of Mechanical Engineering

Delhi Technological University,

Delhi – 110042

August, 2023

DELHI TECHNOLOGICAL UNIVERSITY

(Govt. of National Capital Territory of Delhi)
BAWANA ROAD, DELHI – 110042

CERTIFICATE

This is to certify that the work embodied in the research plan entitled **"THERMODYNAMIC ANALYSIS OF SOLAR BASED POLYGENERATION SYSTEM FOR A RESIDENTIAL COMMUNITY"** has been completed by Mr. **FAIZAN KHALID (Roll No.- 2K19/PhD/ME/19)** under the guidance of Prof. Rajesh Kumar, Professor, Department of Mechanical Engineering, DTU, towards partial fulfilment of the requirements for the degree of Doctor of Philosophy of Delhi Technological University, Delhi. This work is based on original research and has not been submitted in full or in part for any other diploma or degree of any university.

Prof. Rajesh Kumar
Professor
Dept. of Mechanical Engineering
Delhi Technological University, Delhi

ACKNOWLEDGEMENT

First of all, I am highly indebted and thankful, to Almighty Allah, the most merciful and benevolent to all, who thought man that which he knew not and bestowed the man with epistemology and gave him the potential to ameliorate the same. It is his blessing, which inspired and enabled me to complete this work. It is my pleasant duty to acknowledge the help received from several individuals during this work.

It is my great pleasure to express my profound gratitude to my guide **Prof. Rajesh Kumar**, Professor, Department of Mechanical Engineering, DTU for his illuminative and precious guidance, constant supervision, critical opinion and timely suggestion, constant beneficial encouragement and technical tips which have always been a source of inspiration during the preparation of the thesis. His valuable comments and advice gave me the confidence to overcome the challenges in formulating this thesis.

I pay my sincere thanks to **Prof**. **S.K. Garg**, Head of the Department and DRC Chairman (Dept. of Mechanical Engineering), for giving me an opportunity to do research. I am thankful to all faculty members and technical staff of the department for their guidance and help.

Last but not least, I would like to express my special thanks to my parents, wife, and brothers for their tremendous support, continuous motivation, unconditional love, and encouragement throughout the years.

FAIZAN KHALID
(Roll No.- 2K19/PhD/ME/19)
Delhi Technological University
Delhi-110042

ABSTRACT

Electricity generation using renewable energy helps in combating the emissions produced by fossil fuel-based units. One such renewable energy source which can be utilized more effectively is solar energy and it is one of the finest accessible choices for fighting the issues of increasing electricity use, fossil fuel depletion, and global warming because it is available freely and abundant. However, there are some limitations with solar energy-based systems and one of them is their intermittency in operation as solar energy is not accessible throughout the day and does not remain the same throughout the year. Utilization of solar energy to generate electricity, cooling, and freshwater, hydrogen (as an energy source) in remote areas in a sustainable way still poses lots of challenges to researchers because of poorer conversion efficiencies. The goal of the current work is to design new solar-operated systems to produce electricity, cooling, hydrogen, and fresh water in remote areas. Thus, in this thesis, three solar energy-based systems (solar heliostat system, parabolic trough collector (PTC) operated polygeneration system, and solar-operated trigeneration system) for the self-sustained community are presented and evaluated by thermodynamic principles using energy and exergy analyses for technical feasibility. Parametric study of each system individually would help to understand the impact of design factors on the systems performance.

System 1 is a solar heliostat system (based on molten salt) that can meet out the electricity demand, hydrogen (for the refuelling of the vehicles) and cooling load in a community in remote areas. Steam Rankine cycle is utilized to feed the electrical power demand while some of the steam is bleed out to operate the two-stage ammonia water-based absorption system for cooling application. The result of the System 1 shows that with a heliostat area of 6000 m^2, 372 kW of electricity, 610 kW of cooling capacity, and 7.2 kg/h of hydrogen is generated. Furthermore, results of exergy study reveals that the significant exergy is being destroyed in the central receiver (1170 kW) followed by heliostat (980 kW). The performance evaluation of the presented system is made via exergy and energy efficiencies and estimated as 17.7%, and 38.9% respectively. Effects of some crucial parameters such as direct normal irradiance, evaporator temperature, the bleeding ratio etc. have been studied on the overall system performance. It has been found that 55% of useful exergy is being destroyed in the central receiver and heliostat

field. On an average DNI of 700 W/m^2, for a 6 hour day the designed system can provide a cooling capacity of 3 kW to each house with an electrical load of 2 kW. Furthermore, the produced hydrogen can fuel, 100 vehicles with an average range of 100 km per day. Parametric analysis reveals that the central receiver efficiencies increase with an increase in DNI.

System 2 is a new parabolic trough collector (PTC) operated polygeneration system that is used to produce freshwater, hydrogen, cooling, and electricity in a residential society. Dowtherm A (a heat transfer fluid) is utilized for transferring the heat from PTC to ORC, which is used to produce electrical power. The produced electrical power is utilized in three different ways, namely, to run the home appliances, to generate hydrogen (using water electrolysis), and to produce cooling (through a vapor compression cycle). Vapor compression cycle supplied the cooling to preserve the food, milk, and to operate the freezing desalination process. Effects of several factors, such as direct normal irradiance, evaporator temperature, and seawater inlet temperature, have been analyzed on the overall system behaviour. Thermodynamic study results show that for a PTC area of 2000 m^2, an electrical output obtained is 72 kW, the cooling rate is 112 kW, and the amount of fresh water obtained is 18.4 l/day and 10.8 kg/day of hydrogen for mean solar irradiation of 700 W/m^2. The systems' energy efficiency is computed as 17.5%, and systems' exergy efficiency as evaluated as 10.9%. Simulation results show that on a typical summer day, in India (environment temperature of 35°C, direct normal irradiation of 700 W/m^2), the presented system will give electrical power to a housing society of around 60 houses/apartment (having 250 people) in a sustainable way. Furthermore, the proposed system delivers a cooling rate of 2 kW per house. The analysis also reveals that the rate of exergy destroyed in the parabolic trough collector is extreme leading to poor overall efficiencies of the system.

System 3 is a new solar-operated trigeneration system to provide cooling, electricity, and fresh water using PTCs in remote areas. Electrical power is generated by using ORC, and cooling and fresh water (using freezing desalination technique) is obtained by two-stage NH_3-H_2O vapor absorption system run by solar energy. Simulation results show that for PTC arrays of 200 m^2, an electrical output obtained is 3.3 kW, cooling rate is 20.4 kW, and rate of freshwater produced is 36 kg/h for an average solar irradiance of 700 W/m^2. Additionally, sensitivity analysis is conducted by varying the parameter like solar irradiation, evaporator temperature, seawater inlet temperature etc. and their effect on performance characteristics of the overall setup is

investigated. Analysis reveals that maximum exergy is being wasted in the parabolic trough collectors pursued by HRVG. Simulation results show that the systems' energy efficiency is 18.8% and the systems' exergy efficiency is 4.7%. Additionally, PTCs' exergy and energy efficiencies are calculated as 29.8% and 70%, respectively. Analysis also reveals that PTC has an exergy destruction rate of 85.0 kW.

In overall, each system has its own merits and demerits and could provide a potential option for solar-dominated remote areas to obtain cooling, freshwater, hydrogen, and electrical power in an environmentally safer manner. It has been observed that System 1 is suitable for the location where sufficient sunshine is available to produce hydrogen, electricity and cooling for a residential community of 200 houses (800 people). However, System 2 can be installed or recommended for the location having sufficient sunshine and scarcity of potable drinking water. The designed system produced four useful outputs namely, electricity, cooling, freshwater and hydrogen for the community of 250 people. While System 3 can be implemented in the location where there is a need of cooling, electricity and freshwater with an abundance of sunshine and source of saline water. Additionally, the results in this thesis clearly shows the importance of hydrogen production in any solar energy system. The result presented in the current thesis may help the designers/researcher to create a self-sustained community in a more environmental and benign manner.

List of Papers Published

1. **Faizan Khalid**, and Rajesh Kumar "Development and assessment of a new solar-based trigeneration system using hydrogen for vehicular application in a self-sustained community" International Journal of Hydrogen Energy, 2022;26082-26090, **(Elsevier, SCIE indexed,** Impact factor:7.2)
2. **Faizan Khalid**, and Rajesh Kumar "Thermodynamic assessment of a new PTC-operated polygeneration system for fresh water, cooling, electricity, and hydrogen production for a residential community" International Journal of Hydrogen Energy, (In Press), **(Elsevier, SCIE indexed,** Impact factor:7.2)
3. **Faizan Khalid,** Rajesh Kumar and Farrukh Khalid "Feasibility study of a new solar based trigeneration system for fresh water, cooling and electricity production" International Journal of Energy Research, 2021;19500-19508 (Wiley, SCIE indexed, Impact factor: 4.672)
4. **Faizan Khalid**, and Rajesh Kumar "A new PTC operated polygeneration system for fresh water, cooling, electricity and hydrogen production for a residential community: A Thermodynamic Assessment" 6th International Hydrogen Technologies Congress (IHTEC-22), 23rd - 26th January 2022, Mechanical Engineering Department, Canakkale Onsekiz Mart University, **Canakkale**, **Turkey (International Conference)**
5. **Faizan Khalid**, and Rajesh Kumar "2E Analysis of Solar Assisted Cogeneration System for Electric Power and Cooling" International Conference on Advances in Heat Transfer and Fluid Dynamics AHTFD-22, 01st - 03th December 2022, Department of Mechanical Engineering, Z.H. College of Engineering & Technology, India (**International Conference)**

TABLE OF CONTENT

LIST OF TABLES

LIST OF FIGURES

NOMENCLATURE

a	freshwater to evaporator ratio
A	Total area (m^2)
C, CR	Concentration Ratio
DNI	Direct normal irradiation per unit area (W/m^2)
ex	Specific exergy (kJ/kg)
$\dot{Ex}$	Exergy rate (kW)
h	Specific enthalpy (kJ/kg)
IR	Ice Ratio
$\dot{m}$	Mass flow rate (kg/s)
$\dot{Q}$	Heat transfer rate (kW)
R	Ice ratio
s	Specific entropy (kJ/kgK)
S	Salinity (%)
T	Temperature (°C)
$\dot{W}$	Work rate (kW)
X	Salinity (ppm)
z	cooling to power ratio

Greek Letters

η	Efficiency (%)

Subscripts

abs	absorber
b	brine
comp	compressor
cond	condenser
d	destruction
desorb	desorber

elec electrolyzer

en energy

evap evaporator

ex exergy

f feed

fw freshwater

ov overall

rect rectifier

sol solar

sw seawater

t turbine

Acronyms

AEME Anion exchange membrane electrolyzer

AWE Alkaline water electrolyzer

HRVG Heat recovery vapor generator

HTF Heat transfer fluid

ORC Organic Rankine cycle

PEME Proton exchange membrane electrolyzer

PTC Parabolic trough collector

RHX Rectifier heat exchanger

SHX Solution heat exchanger

SOE Solid oxide electrolyzer

TRL Technological readiness level

VCR Vapor compression refrigeration

Chapter 1

Introduction and Literature Review

At the current time, electrical energy is primarily produced by using non-conventional sources of energy like natural gas, oil and coal which are not only going to vanish but also release hazardous gases and/or liquid pollutants during operation. In the year 2018, CO_2 emissions by fossil fuels were 33285 million tonnes of oil equivalent (Mtoe) contributing to 99.3% of the total world's, CO_2 emissions (see Table 1.1).

Table 1.1 Global CO_2 emissions in 2018

	Mtoe	%
Fossil Fuels	33285	99.32
Others	228.0	0.68
Total	33513	100.00

Source: [1]

1.1 Solar Energy

Electricity generation using renewable energy can play a vital role in combating the emissions produced by fossil fuel-based units. One such renewable energy source which can be utilized more effectively is solar energy and it is one of the finest accessible choices for fighting the issues of increasing electricity use, fossil fuel depletion, and global warming because it is available freely and abundant [2-4]. Furthermore, solar energy is one of the extremely favorable options in place of fossil fuels for electrical power production. The solar energy could be harnessed by using collectors such as solar photovoltaic, solar concentrator etc. Numerous types of solar collectors like flat plat, evacuated tube is used up to the temperature of 150℃, while concentrating type collectors (parabolic dish type, linear Fresnel collector, solar dish, and heliostat field) can be used for higher temperature (see Table 1.2). One of the matured concentrating collectors is the parabolic trough collectors (PTC) which can be used upto 673 K. There are numerous ways to harness energy from PTC for electrical use. However, due to the improved performance, reliability, usability, low maintenance cost, the organic Rankine cycle (ORC) for electrical power generation is one of the most feasible choice in the medium temperature range upto 523 K [6].

Table 1.2 Various types of solar collector with their operating temperature and uses

Type of solar collector	Type of absorber	Operating temperature range (K)	Uses
Flat plate (air as a working fluid)	Flat	303-348	To heat the space and for drying purposes
Flat plate (water as a working fluid)	Flat	313-358	To heat the water, providing industrial heat, heat for thermal desalination and refrigeration, etc.
Evacuated tube	Flat	323-423	
Compound parabolic	Tubular	333-493	
Parabolic trough	Tubular	333-573	To produce electricity
Linear Fresnel	Tubular	333-523	
Parabolic dish	Point	373-773	
Heliostat field	Point	473-2273	
Photovoltaic thermal (liquid as a working fluid)	Flat	303-353	Cogeneration (heated water and electrical power)
Photovoltaic thermal (air as a working fluid)	Flat	303-338	Cogeneration (heated air and electrical power)

Source: [5]

Furthermore, if the temperature obtained from the sun is more than 400°C, the concentrated solar power (CSP) is considered to be more suitable. Recently, lots of development have been occurred worldwide in the CSP technologies which have parabolic troughs, dish and power towers. However, the conversion efficiencies of the CSP based energy systems is low which leads to increase in the cost of electricity produced, and thus efforts must need to be done so that CSP can be a cost-effective technology. By employing a trigeneration or multigeneration system, the environmental impact may be lowered, and the efficiency of such system could be elevated [7-9]. With the help of cogeneration cycles, the thermal potential of the hotter regions of the world can be explored in a more environmentally benign manner. However, there are some limitations with solar energy-based systems and one of them is their intermittency in operation as

solar energy is not accessible through the day and does not remain same throughout the year [10,11]. However, this limitation can be addressed by using energy storage when there is not enough electricity to meet the peak demand. Figure 1.1 shows various technologies used for energy storage ranging from mechanical to thermal. Various devices such as flywheels, hydrogen, flow batteries can be used for energy storage [12-14]. The renewable energy sources have another issue i.e. storage of excess energy. Energy storage devices can sort out this problem and also helps in reducing the voltage fluctuations [15].

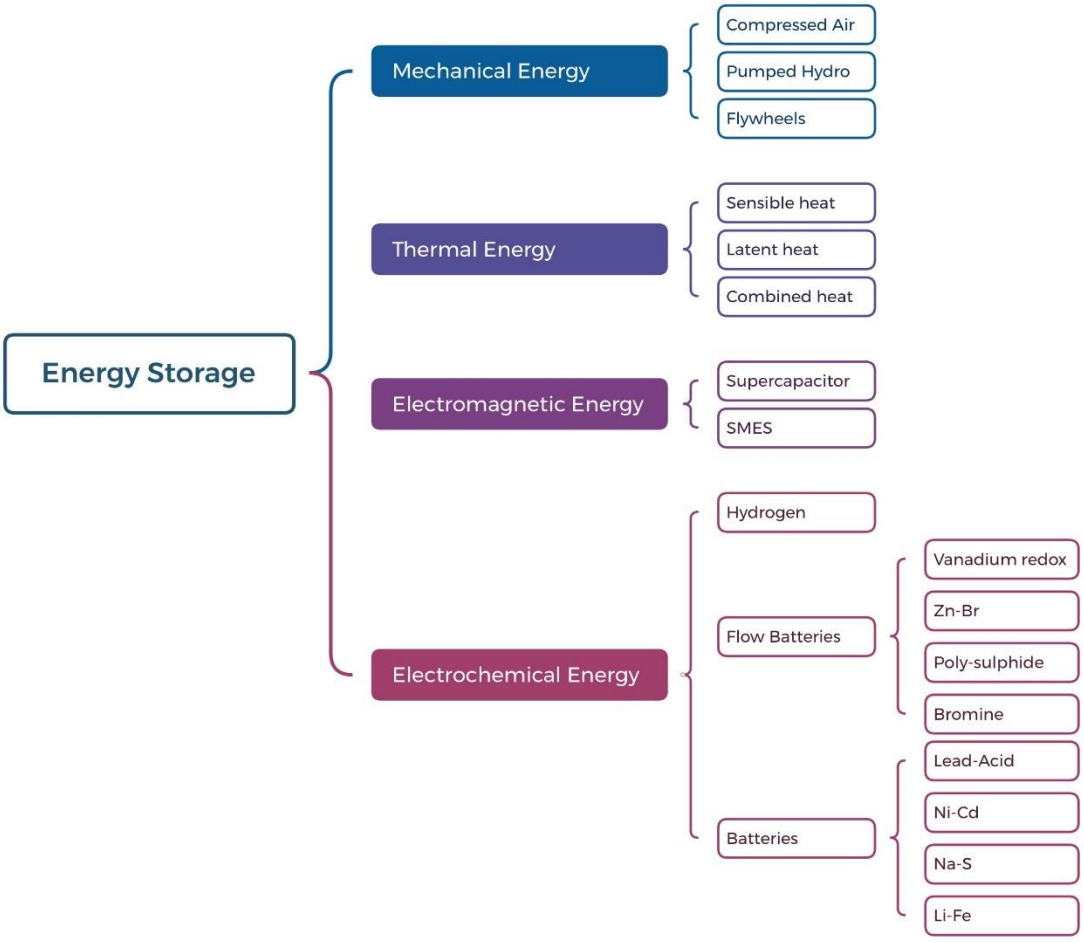

Figure 1.1 Various types of energy storage technologies [12]

1.2 Hydrogen Energy

With the aim of reducing greenhouse gas emissions to net zero, various countries have committed their legal obligations. To achieve this target, several technologies based on renewable energies must be implemented. For instance, the use of hydrogen as an energy vector can play an important role if produced by renewable [16]. Additionally, hydrogen can play a vital role in energy storage and it's recognised that it would lead to improved energy management and better efficiency of energy systems in a sustainable way [17]. The reduction in the price of hydrogen leads to an increase in its global production and utilization in sectors, mainly industrial and transport to 400% by the year 2050. By 2050, India would be one of the main consumers of hydrogen, consuming almost 10% of the world's global hydrogen demand [18]. Till date, the mostly used method for hydrogen production is steam methane reforming. However, researchers are looking for hydrogen production methods that are green as well as sustainable. One of such method can be production of hydrogen using solar energy. There are numerous technologies to produce hydrogen from solar energy (see Figure 1.2).

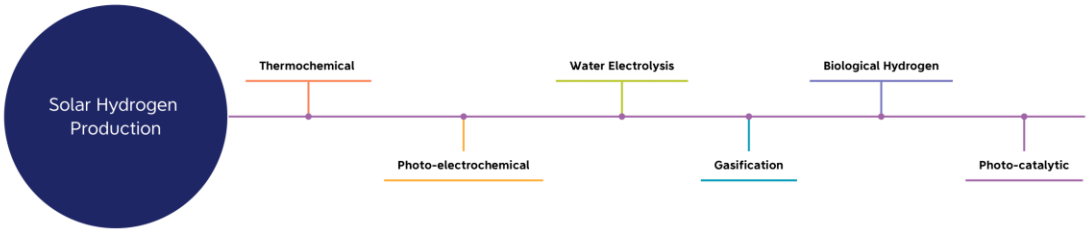

Figure 1.2 Hydrogen production with solar energy (modified from [19])

Water electrolysis using a device called an electrolyzer is one of them. Some of the keys and most suitable electrolyzer technologies that are used worldwide are given in Table 1.3. It is evident from the table that, each one of the technologies has certain advantages and shortcomings. For instance, one can obtain around 99.5% of pure hydrogen using an alkaline water electrolyzer (AWE); however, with the use of a proton exchange membrane electrolyzer (PEME) a purity of more than 99.999% can be achieved. The technological readiness level of AWE is 10 while that of PEM is 9 which shows that AWE is more mature compared to PEM. The PEM has advantage over AWE because of purity of hydrogen produced which makes the

hydrogen produce more suitable for fuel cell applications as small amount of impurity can seriously damage the fuel cells. The new type of technologies like solid oxide electrolyzer (SOE) and anion exchange membrane electrolyzer (AEME) are also showing promising results and can be utilized for future energy needs. It is to be noted from the table that PEME is a good fit for low-temperature energy sources (like PTC) for hydrogen production.

Table 1.3 Comparison of different types of electrolyzer technologies

	Alkaline Water Electrolyzer	**Proton Exchange Membrane Electrolyzer**	**Solid Oxide Electrolyzer**	**Anion Exchange Membrane Electrolyzer**
Type of Electrolyte	30%-50% Potassium hydroxide solution	Pure water	Solid oxide	Pure water, alkali solution
Operating Temperature range (K)	343-363	338-358	873-1273	333-353
Current density (A/m^2)	4000	10000-20000	10000-100000	10000-20000
Energy Efficiency of the electrolysis process (%)	55.0-70.0	70.0-90.0	85.0-95.0	70.0-90.0
Purity of hydrogen produced (%)	more than 99.5	more than 99.999	more than 99.99	more than 99.99
Technology Readiness Level (TRL)	10	9	7	5

Source: [20]

1.3 Water Desalination

In addition to clean energy, access to clean water is one of the key challenge encountered by mankind these days. The freshwater can be obtained by purifying the abundant seawater. Numerous techniques for desalination of seawater or brackish water (see Figure 1.3) have been

proposed and studied for freshwater generation ranging from multistage desalination, reverse osmosis, freezing-defreezing etc [22-24].

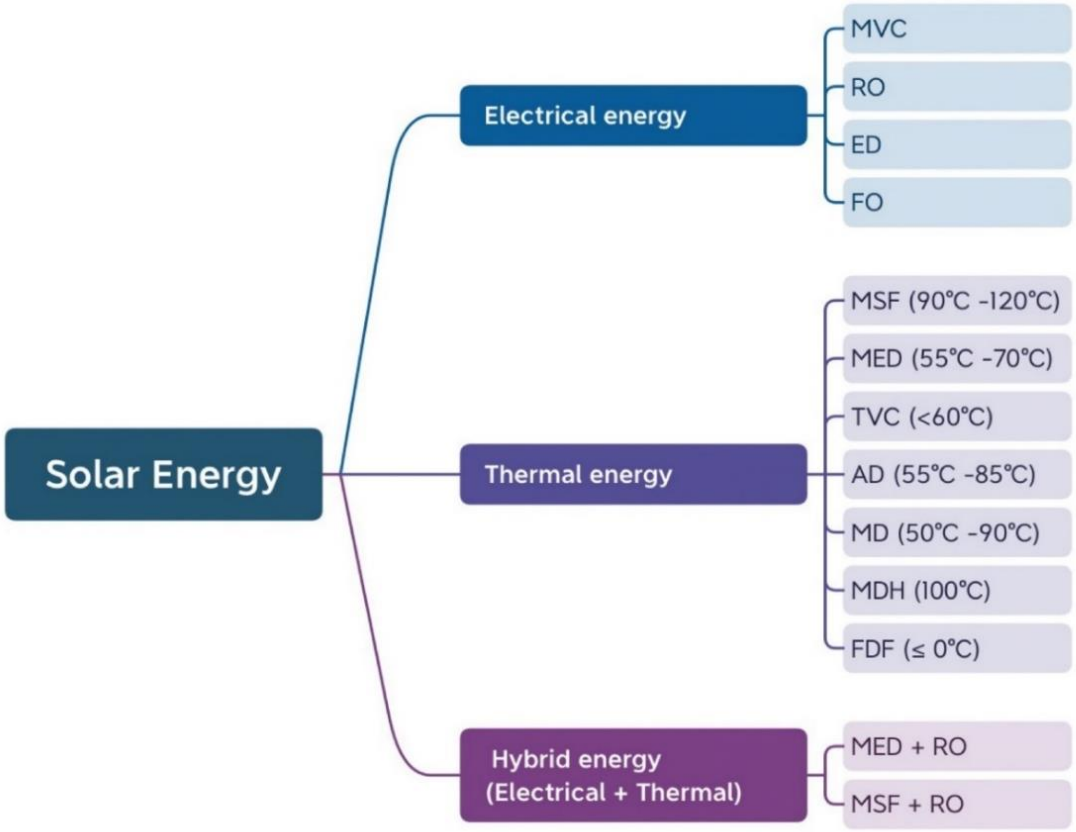

AD = Adsorption Desalination	MSF = Multi stage Flashing
ED = Electro Dialysis	MVC = Mechanical Vapor Compression
FD = Forward Osmosis	RO = Reverse Osmosis
MD = Membrane Desalination	TVC = Thermal Vapor Compression
MED = Multi effect Desalination	FDF = Freezing De-freezing

Figure 1.3 Various technologies for seawater or brackish water using solar energy (modified from [21])

Table 1.4 Comparison of various desalination technologies

Type of desalination technology	Electrical energy requirement (kWh/m^3)	Thermal Energy requirement (kWh/m^3)	Salinity of feedwater (ppm)	Salinity of obtained water (ppm)	Carbon dioxide emissions (kg/m^3)
Reverse Osmosis	8.2	-	45000	10	3.8
Multi-Stage Flashing	5.2	19.4	70000	10	5.5
Multi-Effect Desalination	3.8	16.4	45000	10	6.9
Freezing-Defreezing	11.9	-	37000	100	5.5

Source [25-28]

Table 1.4 provides the comparison of various desalination technologies and it can be concluded from the table that freezing-defreezing technique is a good candidate for desalination as it can handle upto water with a salinity of 37000 ppm. Freezing technique is a quite cost-effective way to produce freshwater [25]. Various investigators have studied freezing desalination technique. For instance, Atia [29] has studied a R-22 operated vapor compression based freezing desalination process found that desalinated water produced by freezing is cost effective. Furthermore, its cost can be reduced by employing solar operated vapor absorption system. One of the available vapor absorption systems to freeze seawater can be achieved by two-stage NH_3-H_2O absorption as it provides temperature below zero degrees using low-grade heat.

Utilization of solar energy to generate electricity, cooling, and freshwater, hydrogen (as an energy source) in remote areas in a sustainable way still poses lots of challenges to researchers due to poorer conversion efficiencies. The goal of the current work is to design new solar-operated systems to produce electricity, cooling, hydrogen, and fresh water in remote areas.

1.4 Literature Review

1.4.1 Type of Solar based Polygeneration Systems

There are several based polygeneration system using solar energy have been investigated by various researchers in the past. Meng et al. [30] have studied the evacuated tube collector based energy system for heating, cooling and electrical power. Their system comprises of organic Rankine cycle, storage tank and evacuated tube collector Ghasemi et al [31] studied a parabolic trough system having Rankine cycle, biomass boiler, desalination unit for cooling, electrical power, LNG and other useful outputs. Rokni [32] has proposed a system comprising of a solar dish, solid oxide fuel cell, desalination system for freshwater, electricity, and hydrogen. They have used Stirling dish engine for conversion of solar energy to useful electrical power. Bai et al. [33] proposed a solar tower based cogeneration system for methanol and electrical power production. Rankine cycle and gas turbine cycles are the heat engines used in their analysis along with components like distillation unit, heat exchangers. Irrespective of the type of the system proposed, the efficiencies of such systems is greatly depend upon operating temperature, solar irradiation, environmental temperature etc. Thus, a proper thermodynamic investigation is needed for better assessment.

1.4.2 Thermodynamic Analysis of Solar based Polygeneration Systems

The solar operated polygeneration systems can be primarily divided into two main sub categories namely; PTC based and Heliostat based. Following sections give the literature pertaining to both the technologies.

a) Polygeneration system with PTC

There are numerous solar-based energy systems, however, PTC is considered one of the efficient and cost-effective ways in the operating range of 50℃-400℃ [6,34]. Furthermore, the utilization of PTC using the Organic Rankine Cycle for electricity production is considered an efficient and best suitable method up to 250℃ [6]. Various types of ORCs' working fluids for PTC have been analyzed by Quoilin et al [35]. They have suggested that the functioning of ORC is greatly altered by the temperature ranges of working fluids. Furthermore, they have suggested that refrigerants like R717, R134a, R600a, and R141b are among the best suitable for the temperature

upto 250℃. Fernández-Guillamón et al. [36] have also studied various working fluids for the ORC and suggest that their behavior is mainly influenced by the turbine inlet temperature. Similarly, Tchanche et al. [37] studied around 20 fluids for low-temperature ORC applications and suggest that ammonia (R717) is an efficient working fluid due to its high boiling point. Al-Sulaiman et al. [38] studied a combined cooling, heating, and power novel setup having PTCs and an ORC. They have studied the effect of various parameters like inlet pressure of the turbine, ORC evaporator pinch point temperature and inlet temperature of ORC pump. Al-Sulaiman et al. [39] conducted the thermodynamic analysis of a power systems operated on PTCs. It was found that PTC accounts for exergy destruction around 70%, while in evaporator it is 13%.

Pourmoghadam and Kasaeian [40] have studied recently the PTC based mulitgeneration system through energy and economic point of view. They have subcomponents ORC, MED unit, PTC, ejector cooling, and PCM storage unit. Khalid et al. [41] have studied a multigeneration system for freshwater, electricity, and cooling comprising ORC run by solar energy.

b) Polygeneration system with solar tower

In solar tower powered polygeneration system, the concentrating ratio is quite high usually more than 500. Several studies have been conducted and reported for polygeneration system with solar tower. For instance, Xu et al. [42] performed the exergy and energy analyses of solar powered energy generation system using Rankine cycle. They have seen the effects of various parameters such as direct normal irradiation (DNI), concentration ratio on the performance of the system. They have found that central receiver has the maximum exergy destruction rate followed heliostat field. The exergy destroyed in the steam generation cycle is significant. Pelay et al. [43] done the thermodynamic study of a solar tower-based Rankine cycle for electrical needs. They have used exergy and energy principle in their assessment. Jaubert et al. [44] carried out the exergy and energy assessment of solar operated multigeneration system producing freshwater and electricity. They have used concentrated solar power based organic Rankine cycle for power production, and freshwater by using combination of reverse osmosis and multi-effect desalination processes. Hamilton et al. [45] discusses the concentrated solar power plants for power generation using heat transfer fluid (molten salt) from the receiver to the steam generator. They have used a software called system advisor model in their assessment and conclude that cycle system performance greatly affected by molten salt inlet temperature, mass flow rate and

ambient temperature. Recently, Azzam and Dincer [46] design an integrated solar energy system for smart cities. They have considered combination of concentrated solar power and photovoltaic thermal for power generation. They used exergy analysis in their assessment and conclude that exergy destruction rate by the concentrated solar power contribute to the most. Tukenmez et al. [47] have proposed a hybrid system having solar and biomass for ammonia and hydrogen generation. Their results show that one achieves mass flow rate of ammonia and hydrogen as 1200 kg/h, and 308 kg/h respectively under designed conditions. Rovense et al. [48] have carried out the thermoeconomic analysis of a 150 MW solar based power plant. They have optimized the number of solar towers, size, and design for different dispatch scenarios. Kahraman and Dincer [49] evaluated a solar operated energy system for multigeneration application using waste heat as one of the key components. They have reported an overall exergy efficiency of 56.4% and energy efficiency of 61.1%. Alirahimi et al. [50] proposed and study a heliostat based solar energy system incorporating biomass. They have achieved an optimized exergy efficiency of 26.7% using artificial neural network method.

1.4.3 Hydrogen Production Systems

Globally researchers are looking for systems that can produce hydrogen in a sustainable manner without causing much less damage to the environment. Here, a summary of the key studies in the area of hydrogen production (mainly PEME) is presented.

Recently, Yilmaz et al. [51] have studied a multigeneration system in which they have produced many useful outputs namely; freshwater, cooling, hydrogen, electricity and heating. They have used supercritical CO_2 based Brayton cycle and transcritical Rankine cycle as heat engine for converting solar energy into electricity. Bozgeyik et al. [52] have proposed and thermodynamically studied a multigeneration system for freshwater, hydrogen, and electricity using PTC comprising ORC. Their simulation results show that one can obtain 20.39 kg per day of hydrogen under design conditions. Additionally, freshwater of 5740 liters per day can also be produced. Yuksel et al. [53] designed and analyzed a multigeneration system that runs on solar energy (based on PTC) for electricity, methane, ammonia, and urea production. They have performed exergy and energy analyses of the system for its technical feasibility. Results show that with the increase in solar radiation, hydrogen production rate increases, and cost significantly reduces. Derbal-Mokrane et al. [54] studied a parabolic trough collector-based

ORC system for hydrogen production in an Algerian Sahara. They have concluded that the proton exchange membrane (PEM) electrolyzer performs better than the alkaline electrolyzer. Their results show that one can produce 36 kg/h of freshwater under design conditions. Yilmaz et al. [55] have used PTC collectors for various useful outputs like hydrogen, ammonia etc. using a transcritical cycle as the heat engine. Togyhani et al. [56] considered a PV system that gets cooled by nanofluid and utilized to produce hydrogen solar cooling via an absorption cooling cycle. They have studied their system via energy and exergy analyses. Yuksel [57] has proposed and analyzed a thermodynamic system having components namely PTC, ORC, vapor absorption system and PEM electrolyzer.

1.4.4 Economical and Environmental Benefit of Solar based Polygeneration Systems

There are various environmental and economical benefit associated with the solar based polygeneration systems. For instance, Abdelhay [58] proposed a PTC based polygeneration system for freshwater, cooling and electricity and have assessed it thermoeconomically. They predicted that the polygeneration system could led to lowest unit price of water production (1.247 USD/m^3).

Calise et al. [59] analyzed the solar tube collector system with MED desalination for freshwater, heating and cooling. Their results show that the payback period for the proposed system is 3 years. Furthermore, their analysis reveals that by increasing the solar collector to 1200 m2, the payback period can be reduced to 2.4 years. Ghorbani et al [60] studied the solar geothermal based polygeneration system for bio LNG, freshwater, heating and electricity. Their economic analysis shows that the product cost reached 0.5 USD/kWh making a saving of 783.3 MMUS$ per year.

Vazini and Manesh [62] studied the economic and environmental analysis of a solar PTC based polygeneration system having MED, TVC and RO system. Their optimisation results show that the total cost and environmental impact rate of the system decrease by 47.4 USD/h and 49.2 pts/h.

Keshavarzzadeh et al. [62] performed technical, economic, and environmental studies of a hybrid system including a solar tower and desalination unit. Their results show that by using a heliostat field one can reduces CO_2 emission by around 28 %. Esmaeillon et al. [63] have studied a novel

polygeneration system having useful outputs such as electric power, heating, cooling, freshwater and hydrogen. Their results show that the environmental damage effectiveness and sustainability index for the system was 9.01 and 1.29, respectively.

1.4.5 Integration of Polygeneration Systems

Polygeneration systems are those which can produced three useful outputs and are employed to enhance or the extend the efficiencies benefitted offered by cogeneration systems. They are seeming as an extension of cogeneration system in which portion of heat energy, electrical energy or cooling to be used for useful outputs such as hydrogen, freshwater, drying, hot water etc. The design of an effective polygeneration is quite complex in nature as it requires the integration of different energy processes and devices all together for effective and efficient delivery. Various techniques and tools are required to achieve this integration which includes thermodynamic analysis (primarily exergy analysis), economic analysis and environmental impact [64]. Before implementation of polygeneration system for practical applications, all the above mention analysis need to be carried out.

1.5 Research Gaps

From the above literature review, it is clearly shown that currently researchers are reporting the use of solar tower based integrated energy system for multiple useful outputs such as hydrogen, electricity, cooling etc. However, very few have incorporated the two-stage ammonia-based refrigeration system for cooling and barely one has considered the bleeding of steam to run it.
The main research gaps can be summarized as follows:

1. Design of solar powered energy system integrated with Rankine and two-stage ammonia-based refrigeration system for cooling and freezing defreezing applications is limited.
2. Detailed component wise thermodynamic analysis of a solar powered integrated with Rankine and two-stage ammonia-based refrigeration system for cooling and freezing applications is limited.
3. Design of a hydrogen production system for using PTC or solar tower technology is limited for community and vehicular applications.

4. Technological assessment via exergy analysis of such system/s is limited.

1.6 Objectives of the thesis

The main objective of the present thesis is to employs solar energy driven system/s for polygeneration applications (e.g., producing cooling, electricity, and hydrogen etc) for a self-sustained community.

The key objectives of the current study are below:

- To propose and develop the solar based energy systems for production of freshwater, cooling, and electricity incorporating molten salt, Rankine cycle, and absorption cycle for a residential community.
- To employ freezing technique for desalination of seawater run by evaporator of two stage NH_3-H_2O absorption system.
- To develop and assessed a new solar based trigeneration system using hydrogen for vehicular application in a self-sustained community.
- To propose and study a polygeneration system utilizing solar energy via parabolic trough collector (PTC) for freshwater, hydrogen, electricity, and cooling for a society in a remote area

1.7 Organization of the thesis

The current thesis is divided into five chapters. *Chapter 1* provide the overview of solar energy technology for energy harvesting with various hydrogen production methods. Literature pertaining to thermodynamic analysis of solar-based energy systems for polygeneration, and hydrogen production (mainly PEM technology) is also presented in this chapter. This chapter closes with research gaps and objectives of the thesis. *Chapter 2* presents the development and assessment of a new solar based trigeneration system using hydrogen for vehicular application in a self-sustained community. The presented system can meet out the electricity demand, cooling load, and hydrogen (for the refuelling of the vehicles) in a community by using solar heliostat system (based on molten salt) in remote areas. Effects of some crucial parameter such as direct normal irradiance, evaporator temperature, bleeding ratio etc. have been studied on the overall

system performance in this chapter. *Chapter 3* provides a thermodynamic assessment of a new PTC operated polygeneration system for cooling, hydrogen production, fresh water, and electricity for a residential community. *Chapter 4* provides the feasibility study of a new solar based trigenration system for fresh water, cooling, and electricity production. Furthermore, sensitivity analysis is conducted by varying the parameter like solar irradiation, evaporator temperature, seawater inlet temperature etc. and their effect on performance characteristics of the overall setup is investigated in this chapter. *Chapter 5* provides the conclusion of important findings of the current thesis along with the recommendations for future work.

Chapter 2

Development and assessment of a new solar based trigeneration system using hydrogen for vehicular application in a self-sustained community

In the present work, a new solar operated energy system for a self sustained community is presented and analysed via the principles of thermodynamics. The presented system can meet out the electricity demand, cooling load, and hydrogen (for the refuelling of the vehicles) in a community by using solar heliostat system (based on molten salt) in remote areas. Steam Rankine cycle is utilized to feed the electrical power demand while some of the steam is bleed out to operate the two-stage ammonia water-based absorption system for cooling application. The result of the present study shows that with a heliostat area of 6000 m^2, 372 kW of electricity, 610 kW of cooling capacity, and 7.2 kg/h of hydrogen is generated. Furthermore, results of exergy analysis reveals that the maximum exergy destruction takes place in the central receiver (1170 kW) followed by heliostat (980 kW). The performance assessment of the overall presented system is made via exergy and energy efficiencies and estimated as 17.7%, and 38.9% respectively. Effects of some crucial parameter such as direct normal irradiance, evaporator temperature, bleeding ratio etc. have been studied on the systems' performance.

2.1. System Description

A solar operated system for generating cooling, and hydrogen and electricity for a self sustained community is schematically shown in Figure 2.1. This trigeneration system comprises of solar tower-based heliostat system, central receiver, Rankine cycle, vapor absorption system (using two-stage ammonia-water vapor absorption), and electrolyzer. Sun radiation falls on the heliostat field and gets reflected to the central receiver. Molten salt (60% $NaNO_3$-40% KNO_3) enters the central receiver at state 3 and gets warmed from the heat received in the central receiver. The heated molten salt goes to HRSG (heat recovery steam generator) at state 1 and exit at state 2. The heat transfer by the molten salt is utilized to generate the vapor in the HRSG. The generated vapor or steam gets expanded in turbine at state 5 to produce the mechanical power. A portion of the steam is bled at state 10 to run the two-stage vapor absorption system. Steam exits from the turbine at state 5 and gets condensed at state 6 in the condenser 1. Condensate at state 6 enters the pump 1 and gets pressurized. Pressurize condensate (water) gets to the mixing chamber and merged with the bleed steam (state 48) coming out of the Desorber2. A portion of the electrical power obtained from the turbine at state 44 goes to the electrolyzer where it generates hydrogen (at state 46) and oxygen at state 42. The produced hydrogen is sent to the fuel station and used to run the vehicles at state 47. At state 45, useful electricity is feed to the meet the electrical load of

the community and at state 40, the cooling demand of the community is met via the evaporator of the double vapor absorption cycle.

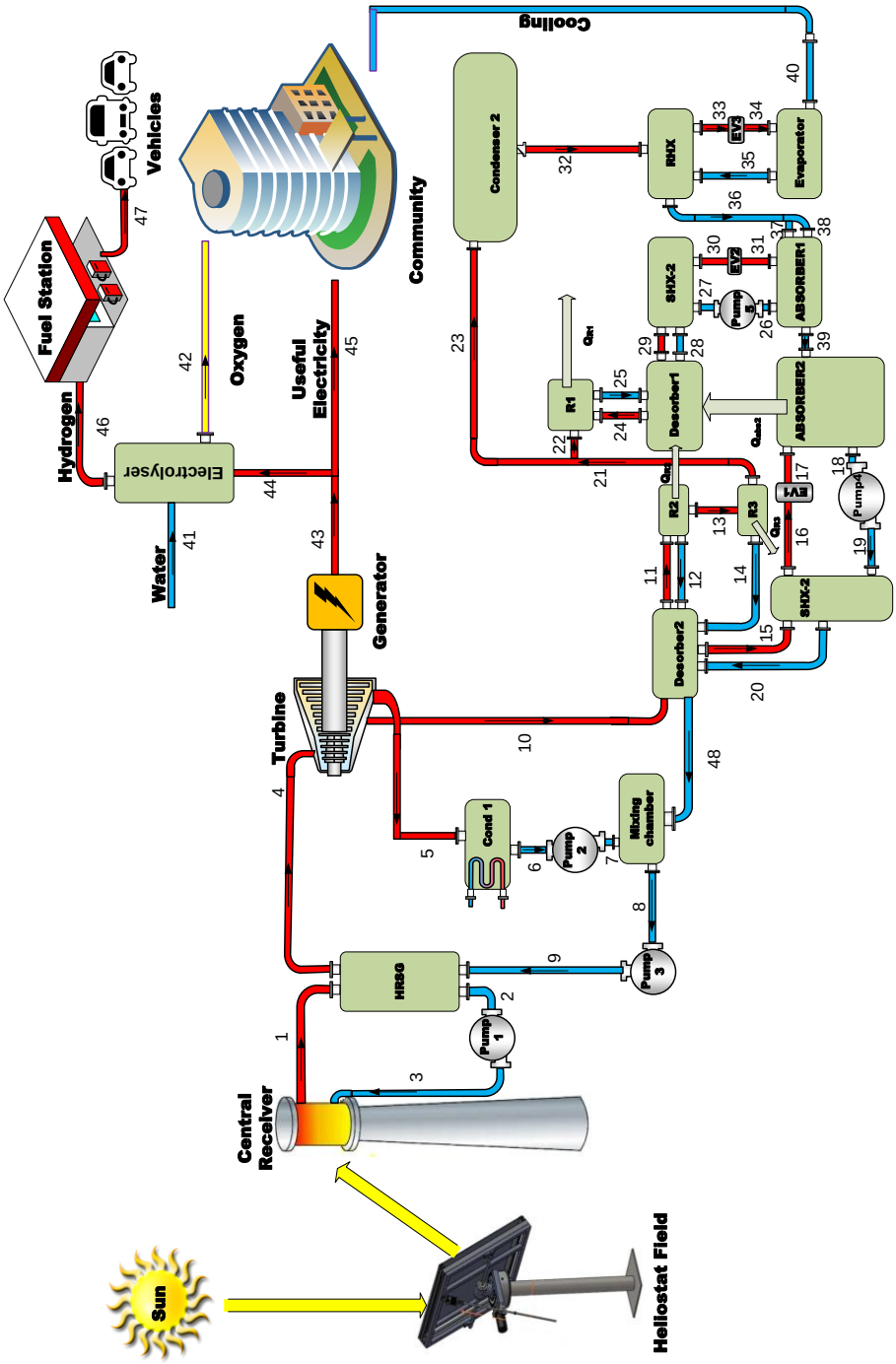

Figure 2.1 Schematic of a solar energy driven trigeneration system for producing cooling, electricity, and hydrogen for a self sustained community

2.2. System Analyses

Technical feasibility of the solar based energy system for a self sustained community presented in previous section (section 2.1) is made via principles of thermodynamics namely, first, and second laws. The following reasonably correct assumptions have been made to ease the analysis:

- Operation of heat exchangers assumed to be adiabatic i.e., with negligible heat loss
- Overall system achieved the steady state
- The pressure losses in the pipelines and network of the overall system are negligible.

Exergy and energy balance rate for the key unit of the system are listed in Table 2.1.

Table 2.1 Exergy and energy balance rate of the key element of the system

Component	**Energy balance rate**	**Exergy balance rate**
Central Receiver	$\dot{m}_3 h_3 + \dot{Q}_{CR} = \dot{m}_1 h_1 + \dot{Q}_{loss,CR}$	$\dot{m}_3 ex_3 + \dot{E}x_{CR}^{Q} = \dot{m}_1 ex_1 + \dot{Q}_{loss,CR}\left(1 - \frac{T_0}{T_{CR}}\right) + \dot{E}x_{d,CR}$
HRSG	$\dot{m}_1 h_1 + \dot{m}_9 h_9 = \dot{m}_4 h_4 + \dot{m}_2 h_2$	$\dot{m}_1 ex_1 + \dot{m}_9 ex_9 = \dot{m}_4 ex_4 + \dot{m}_2 ex_2 + \dot{E}x_{d,HRSG}$
Turbine	$\dot{m}_4 h_4 = \dot{m}_5 h_5 + \dot{m}_{10} h_{10} + \dot{W}_{turbine}$	$\dot{m}_4 ex_4 = \dot{m}_5 ex_5 + \dot{m}_{10} ex_{10} + \dot{W}_{turbine} + \dot{E}x_{d,turbine}$
Desorber 2	$\dot{m}_{10} h_{10} + \dot{m}_{12} h_{12} + \dot{m}_{20} h_{20} + \dot{m}_{14} h_{14} = \dot{m}_{48} h_{48} + \dot{m}_{15} h_{15} + \dot{m}_{11} h_{11}$	$\dot{m}_{10} ex_{10} + \dot{m}_{12} ex_{12} + \dot{m}_{20} ex_{20} + \dot{m}_{14} ex_{14} = \dot{m}_{48} ex_{48} + \dot{m}_{15} ex_{15} + \dot{m}_{11} ex_{11} + \dot{E}x_{d,desorb2}$
Evaporator	$\dot{m}_{34} h_{34} + \dot{Q}_{cooling} = \dot{m}_{35} h_{35}$	$\dot{m}_{34} ex_{34} + \dot{Q}_{cooling}\left(\frac{T_0}{Tevap} - 1\right) = \dot{m}_{35} ex_{35} + \dot{E}x_{d.evap}$
Electrolyzer	$\dot{m}_{41} h_{41} + \dot{W}_{elec} = \dot{m}_{42} h_{42} + \dot{m}_{46} h_{46} + \dot{Q}_{loss,elec}$	$\dot{m}_{41} ex_{41} + \dot{W}_{elec} = \dot{m}_{42} ex_{42} + \dot{m}_{46} ex_{46} + \dot{Q}_{loss,elec}\left(1 - \frac{T_0}{T_{elec}}\right) + \dot{E}x_{d,elec}$

Solar field Analysis

In solar field analysis, quantification of losses in heliostat field, and central receiver are crucial. Amount of heat received by the heliostat is computed as

$$\dot{Q}_{solar} = DNI * A_{field} \quad (2.1)$$

Amount of heat received by the central receiver is calculated as

$$\dot{Q}_{CR} = \eta_{en,helio}\dot{Q}_{solar} \quad (2.2)$$

By the applying the energy balance on the central receiver, the heat loss can be computed as follows:

$$\dot{Q}_{loss,CR} = \dot{Q}_{CR} - \dot{Q}_{abs} \quad (2.3)$$

Losses in the central receiver are mainly of four types namely, emissive, conductive, convective, and reflective heat losses. They are computed using the procedure given by various authors [65,66].

The heat received by the molten salt ($\dot{Q}_{abs}$) is evaluated as

$$\dot{Q}_{abs} = \dot{m}_{salt}(h_1 - h_3) \quad (2.4)$$

The receiver temperature (T_{rec}) can be computed as follows:

$$T_{rec} = T_{ms} + \left[\frac{d_o}{d_i h_{ms}} + \frac{d_o}{2l_k}\ln\frac{d_o}{d_i}\right] \times \frac{\dot{Q}_{CR}F_r C}{A_{field}} \quad (2.5)$$

Performance Assessment

The performance assessment of various component of the system presented in the study is made via exergy and energy efficiencies.

Energy efficiency

Central receivers' energy efficiency is computed as follows:

$$\eta_{en,CR} = \frac{\dot{Q}_{abs}}{\dot{Q}_{CR}} \quad (2.6)$$

The energetic performance of the vapor absorption unit is evaluated as follows:

$$COP_{en} = \frac{\dot{Q}_{evap}}{\dot{m}_{10}(h_{10} - h_{48})} \quad (2.7)$$

Electrolyzers' energy efficiency is computed using following expression:

$$\eta_{en,elec} = \frac{\dot{m}_{46}HHV}{\dot{W}_{elec}} \quad (2.8)$$

where $\dot{W}_{elec} = y \times \dot{W}_{turbine}$, and y is work ratio.

The energy efficiency of the overall system is found using following expression:

$$\eta_{en,ov} = \frac{(\dot{Q}_{evap} + \dot{m}_{46} HHV + \dot{W}_{net})}{\dot{Q}_{sol}} \quad (2.9)$$

Exergy efficiency

The central receviers' exergy efficiency is computed as follows:

$$\eta_{ex,CR} = \frac{\dot{E}x^{Q}_{abs}}{\dot{E}x^{Q}_{CR}} \quad (2.10)$$

The exergetic performance of the vapor absorption system is calculated as

$$COP_{ex} = \frac{\dot{E}x^{Q}_{evap}}{\dot{m}_{10}(ex_{10} - ex_{48})} \quad (2.11)$$

The exergy efficiency of the electrolyzer is computed using following expression:

$$\eta_{ex,elec} = \frac{\dot{m}_{46} ex_{46}}{\dot{W}_{elec}} \quad (2.12)$$

The systems' exergy efficiency is evaluated using following expression:

$$\eta_{ex,ov} = \frac{(\dot{E}x^{Q}_{evap} + \dot{m}_{46} HHV + \dot{W}_{net})}{\dot{E}x^{Q}_{sol}} \quad (2.13)$$

where $\dot{E}x^{Q}_{evap} = \dot{Q}_{evap}\left(\frac{T_0+273}{Tevap+273} - 1\right)$ and $\dot{E}x^{Q}_{sol} = \dot{Q}_{sol}\left[1 - \left(\frac{T_0+273}{T_{Sun}+273}\right)\right]$

2.3 Results and Discussion

The designed system provides the electricity of around 372 kW which will cater the electric power demand of a community of 200 houses/apartment (around 800 people) in an environmentally benign manner on an average sunny day of 6 hrs with an average DNI of 700 W/m^2. Additionally, it can provide a cooling capacity of 3 kW to each house. The produced hydrogen can fuel 100 vehicles with an average range of 100 km per day.

Figure 2.2 illustrates exergy destruction rate of key element of the developed system. It is clearly visible from the figure that central receiver has the largest exergy destruction rate i.e., 29.8% of the available exergy to the system. This is due to the high temperature heat losses (consist of emissive, convective, conductive and reflective heat losses) [67]. Out of available solar exergy, 25% is being destroyed in the heliostat due to poor optical efficiency which is caused by the self shading resulting in the blocking of solar irradiations [68]. The exergy destroyed in HRSG is significant i.e. 6.3% of the available exergy. The contribution to exergy destruction by evaporator and electrolyzer are also significant. Thus, cost effective efforts would be done to

lower these rate of exergy destruction so that better systems' and components' efficiencies can be achieved.

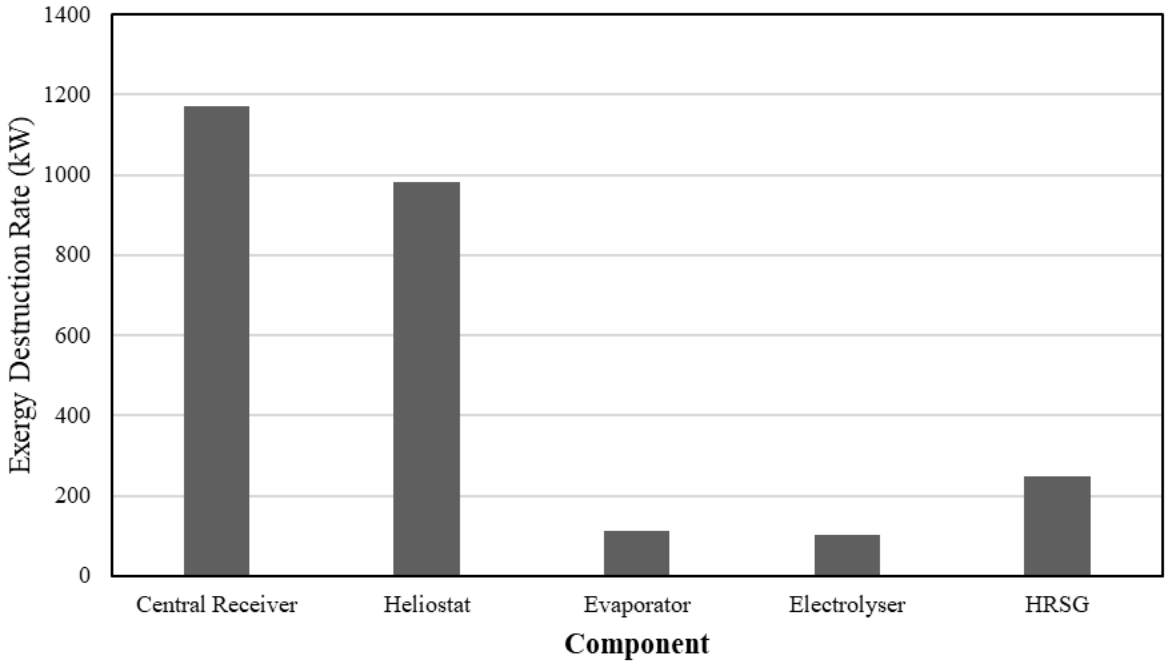

Figure 2.2 Rate of exergy destruction of the key element of the presented system

Table 2.2 lists the parameter used for the heliostat field analysis. It is to be noted from the table that the area of heliostat field consider is 6000 m^2 with a concentration ratio (C) of 800 and view factor (F_r) as 0.8.

Table 2.2 Parameter used in heliostat field analysis

Area of heliostat (m^2)	6000
Concentration ratio, C	800
Passes of tube	20
Number of tubes	10
Fr	0.8
Tube outlet tube (m)	0.01577
Tube inlet diameter (m)	0.01247

Emissivity	0.8
Reflectivity	0.04
Thermal conductivity of metal (W/mK)	24.0
Molten salt thermal conductivity (W/mK)	0.5158

Table 2.3 Input and calculated parameter values

Parameter	**Value**
Net work output rate (kW)	371.6
Electrolyzer work input rate (kW)	371.6
Cooling capacity (kW)	609.6
Systems' energy efficiency (%)	17.7
Systems' exergy efficiency (%)	38.9
Ambient temperature (°C)	20
Evaporator temperature (°C)	-5
Solar irradiation (W/m^2)	700
Sun temperature (°C)	4500
Hydrogen production rate (kg/s)	1.9×10^{-3}
Oxygen production rate (kg/s)	1.6×10^{-2}
Mass flow rate of molten salt (kg/s)	9.0
Bleed ratio, x	0.5
Work ratio, y	0.5
Isentropic efficiency of pump (%)	95.0
Isentropic efficiency of turbine (%)	90.0
Energy efficiency of electrolyzer (%)	76.0
Exergy efficiency of electrolyzer (%)	72.0
Molten salt inlet temperature (°C)	290
Energetic COP	0.61
Exergetic COP	0.158
Central receivers' energy efficiency (%)	85.9
Central receivers' exergy efficiency (%)	56.8

The values of various useful parameters obtained from the analysis of the present system is listed in Table 2.3. From the table one can found that for heliostat area of 6000 m^2, net work rate is 371.6 kW, cooling capacity is 609.6 kW and hydrogen produced is 0.00199 kg/s with the systems' energy and exergy efficiencies as 38.9% and 17.7%, respectively. Furthermore, analysis reveals that 43.2% of inlet exergy to the central receiver is destroyed i.e., exergy efficiency of central receiver as 56.8%. Double stage NH_3-H_2O vapor absorption refrigeration system operates with an energetic COP of 0.61 and exergetic COP of 0.158, under design conditions (see Table 2.3).

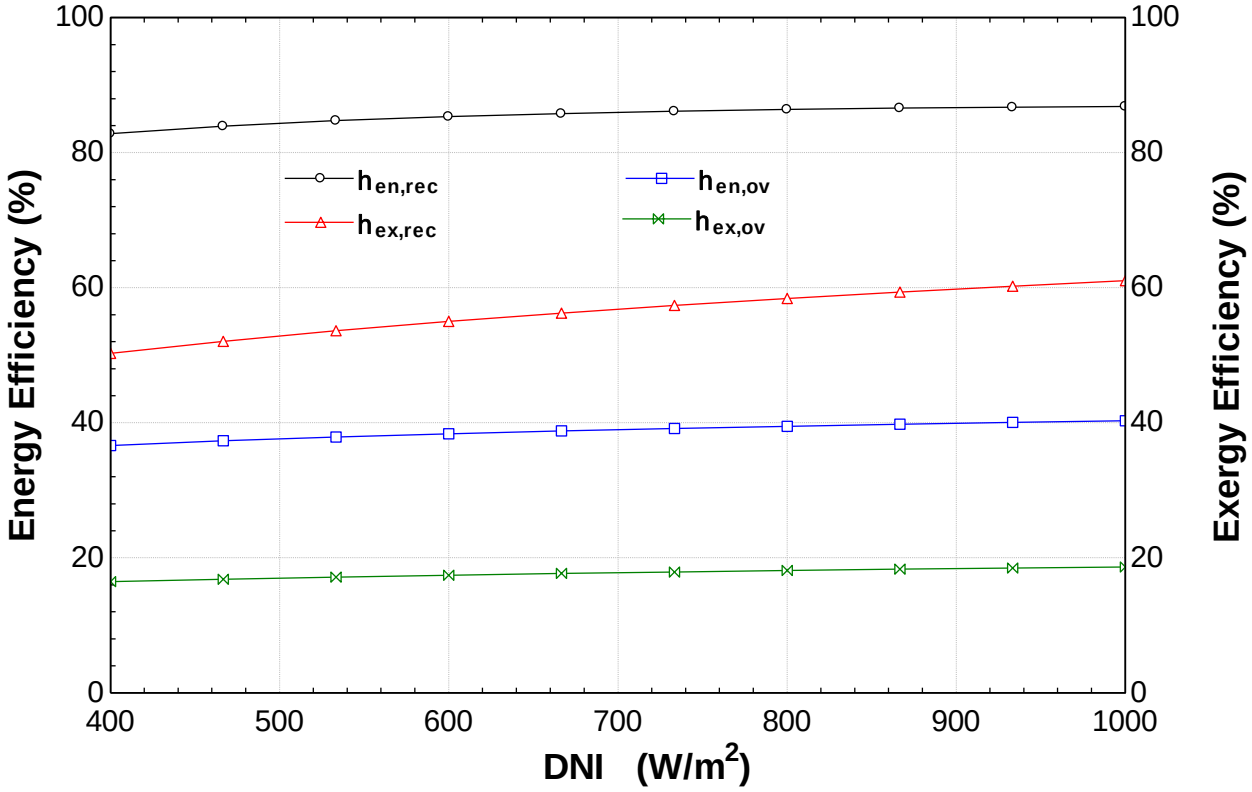

Figure 2.3 Variation of several efficiencies of the system with solar irradiation (DNI)

Figure 2.3 depicts the change in systems' exergy and energy efficiencies and central receivers' exergy and energy efficiencies with the incident solar radiation. With the change in solar irradiance from 400 m^2 to 1000 m^2, the receivers' energy efficiency varies from 82.7% to 86.8% and the exergy efficiency changes from 50.2% to 61.0%. Increase in solar radiation also increases systems' overall energy efficiency from 36.6% to 40.2%, while systems' exergy

efficiency rises from 16.6% to 18.6%. This happens because as the solar irradiance rises, the input energy to the receiver rises and receiver temperature also increase. However, the rate of increase in receivers' temperature is less than the rate at which input energy to the receiver increases resulting in the enhancement of overall efficiencies of the system.

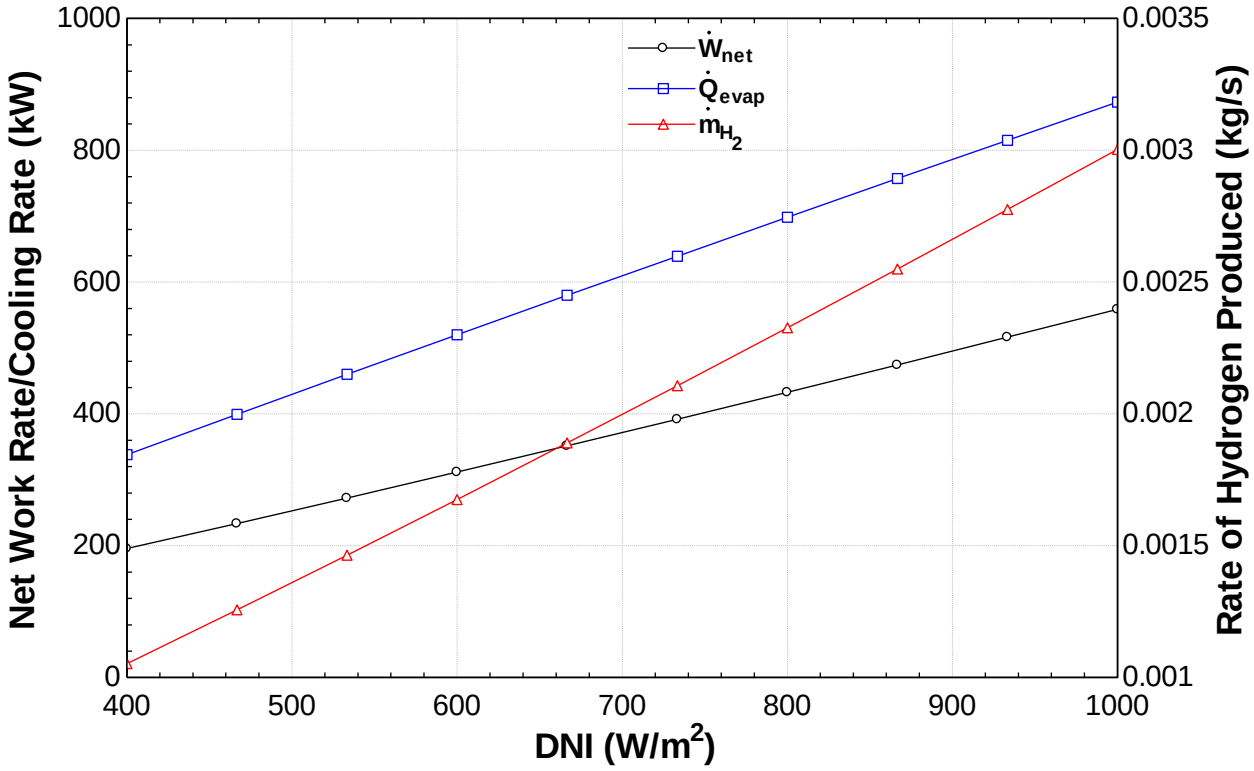

Figure 2.4 Variation of net work rate, cooling rate, and hydrogen produced with solar irradiation (DNI)

Figure 2.4 shows the variation of net work rate, cooling rate, and rate of hydrogen production with the incident solar irradiance. With the change in solar irradiance from 400 W/m^2 to 1000 W/m^2, the net work rate increases from to 195.8 kW to 558.7 kW while cooling capacity rises from 338 kW to 873 kW. The rate of hydrogen generated also rises with the rise in solar irradiance i.e., 0.0019 kg/s to 0.003 kg/s. This happens because as DNI increases, the input energy to the system increases leading to more steam generation causing increase in all the useful outputs.

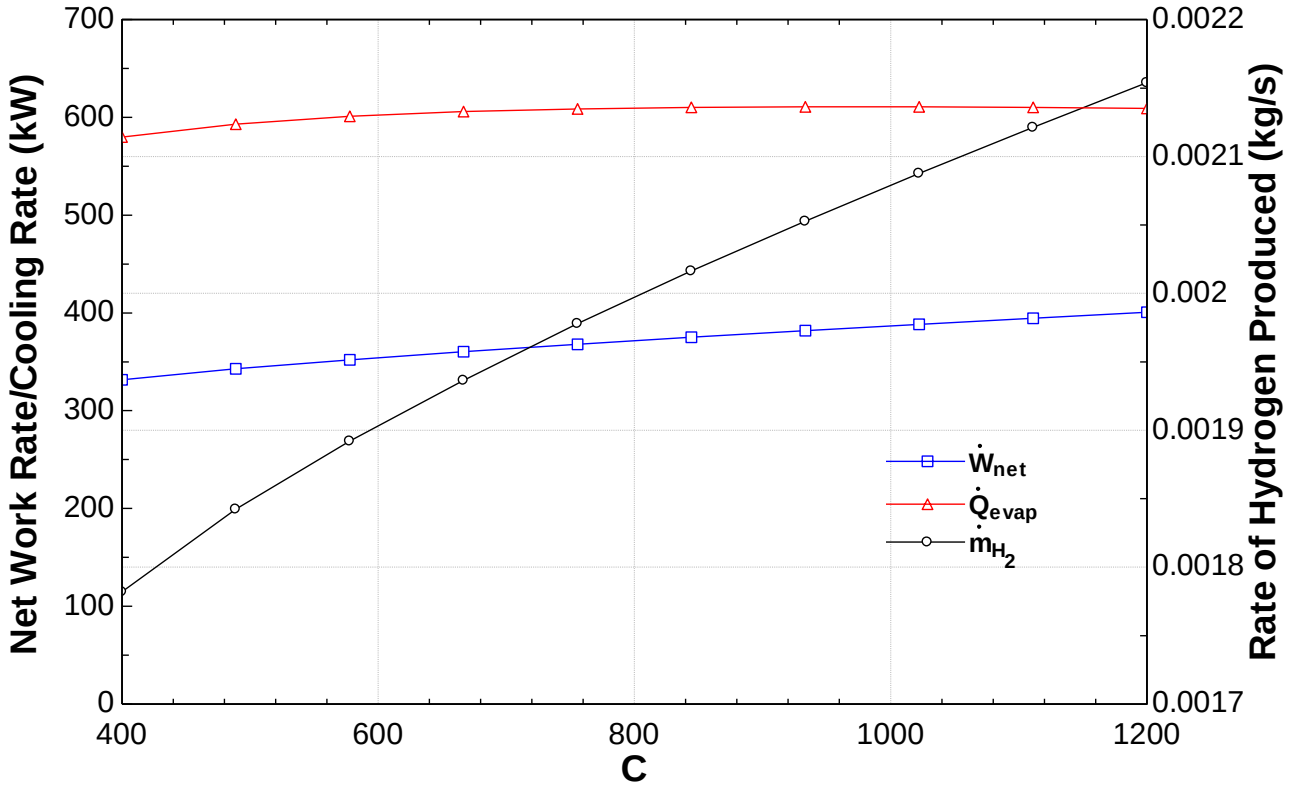

Figure 2.5 Variation of net work rate, cooling rate, and hydrogen produced with concentration ratio

The variation of net work rate, cooling rate, and hydrogen produced with concentration ratio is plotted in Figure 2.5. As the concentration increases from 400 to 1200, the net work rate increases from to 332 kW to 401 kW while cooling capacity changes from 580 kW to 610 kW. The rate of hydrogen production also rises with the rises in concentration ratio i.e., 0.0017 kg/s to 0.0021 kg/s. This happens because as concentration ratio (C) increases, the temperature of the steam generated and receiver temperature would increase resulting in the rise in all the useful outputs.

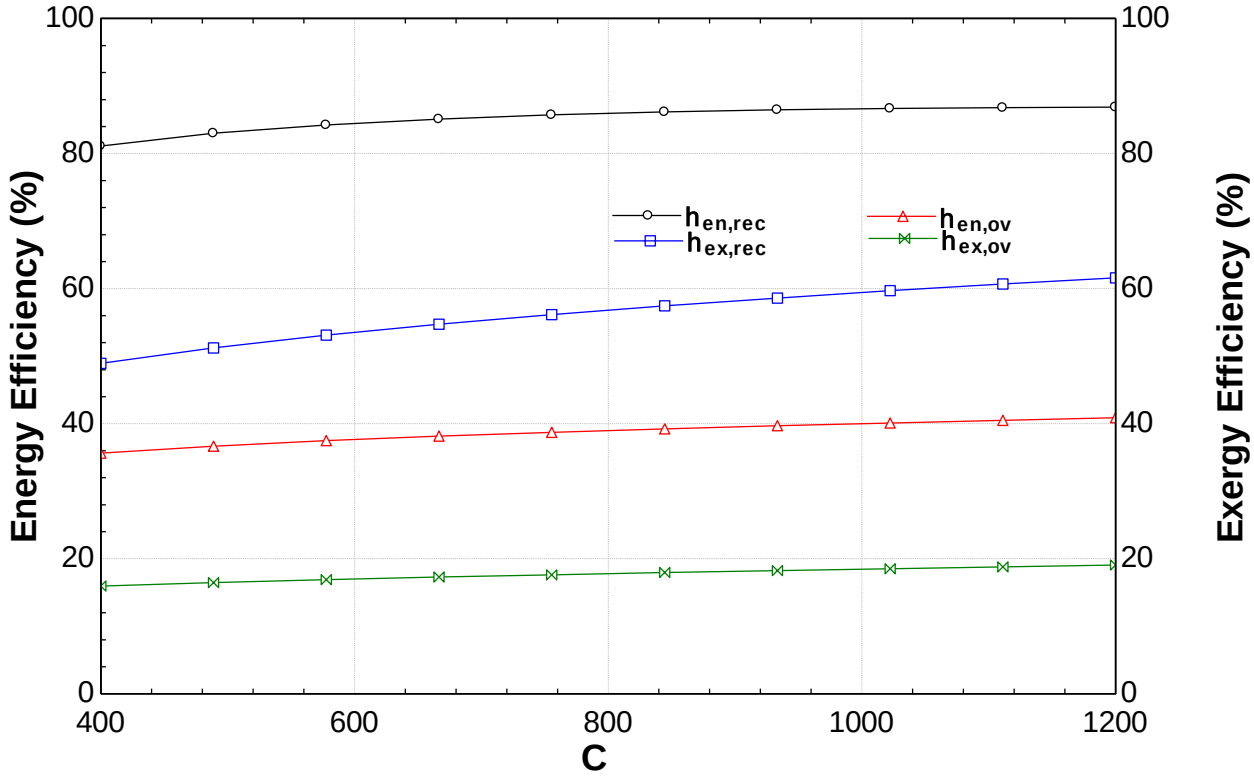

Figure 2.6 Variation of several efficiencies of the system with concentration ratio

Figure 2.6 illustrates the changes in receivers' exergy and exergy efficiencies and overall systems' efficiencies with the concentration ratio. With the rise in concentration ratio, all the systems' efficiencies increase. With the change in CR, the receiver temperature increases and the energy input to the system also rises, thus the systems' efficiencies rises.

With the rise in evaporator temperature from -10℃ to 0℃, systems' overall energy efficiency varies from 36.3% to 41.5%, energetic COP changes from 0.49 to 0.71 and exergetic COP changes from 0.14 to 0.15 while exergy efficiency of the system declines. When the evaporator temperature rises, the amount of cooling capacity rises causing the rise in the overall system, energetic and exergetic COPs. However, systems' exergy efficiency decreases because the thermal exergy of the cooling reduces with the rise in temperature (see Figure 2.7). As evaporator temperature rises, the desorber2 temperature declines, lead to decrease in systems' exergy efficiency (see Figure 2.8). Also, with the increase in evaporator temperature, the cooling obtained by the evaporator increases while the net work obtained by the system remains constant.

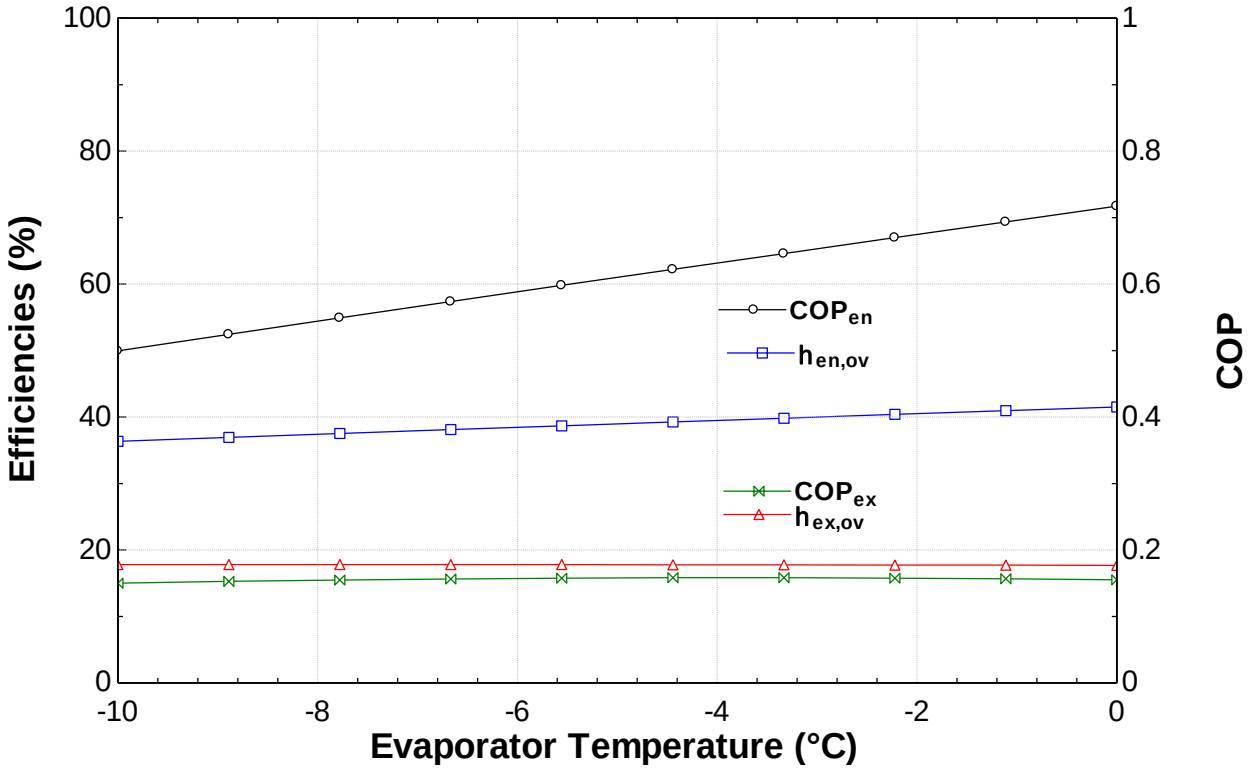

Figure 2.7 Variation of several efficiencies of the system with evaporator temperature

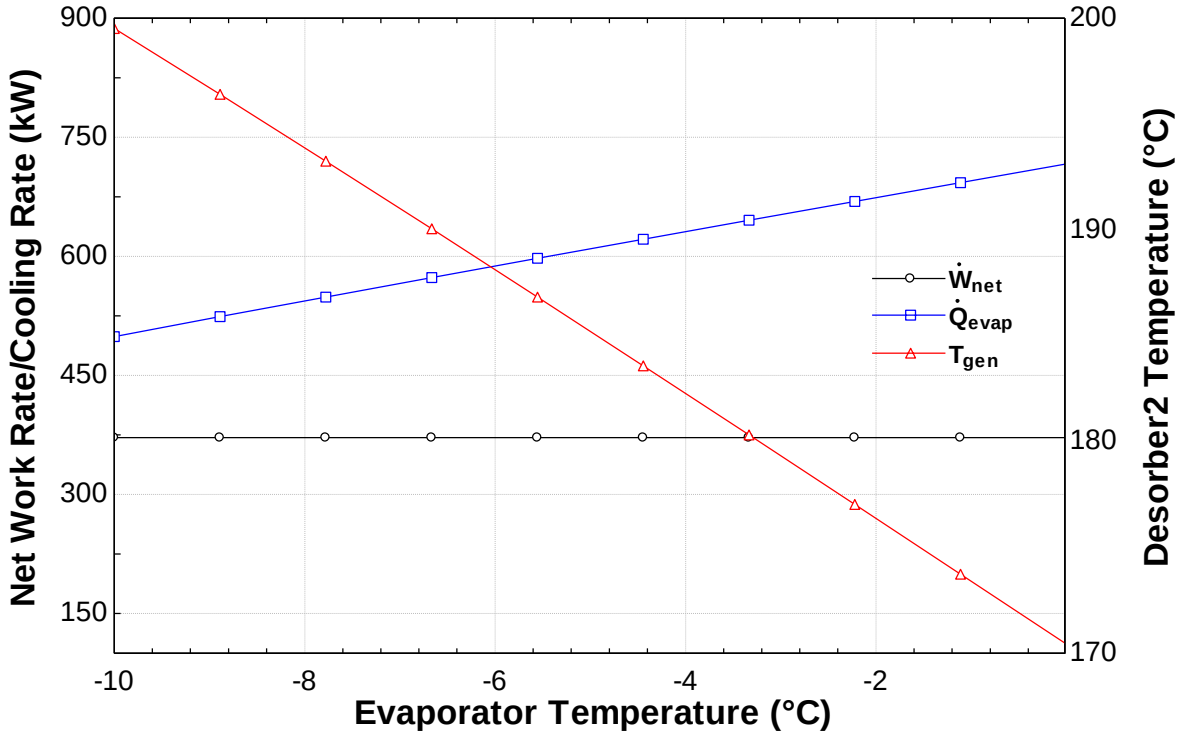

Figure 2.8 Results of evaporator temperature on the net work rate, cooling capacity and desorber2 temperature

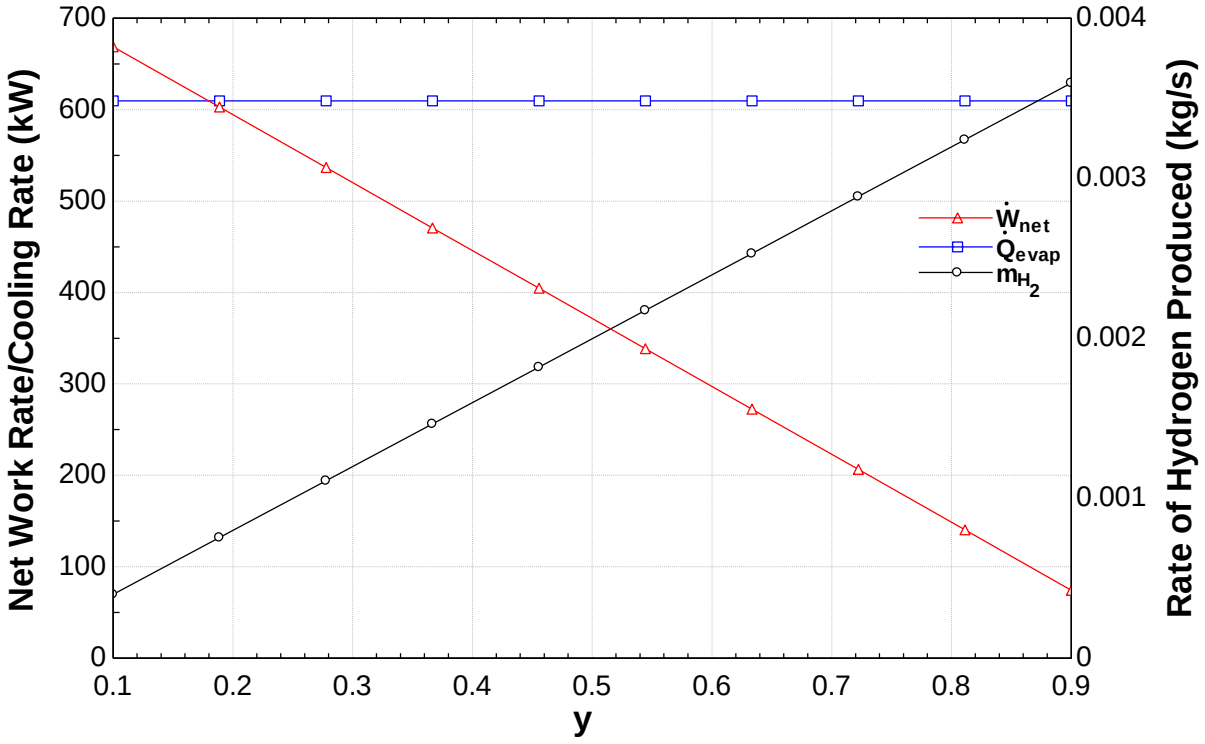

Figure 2.9 Effect of work ratio (y) on the net work rate, cooling capacity and hydrogen produced

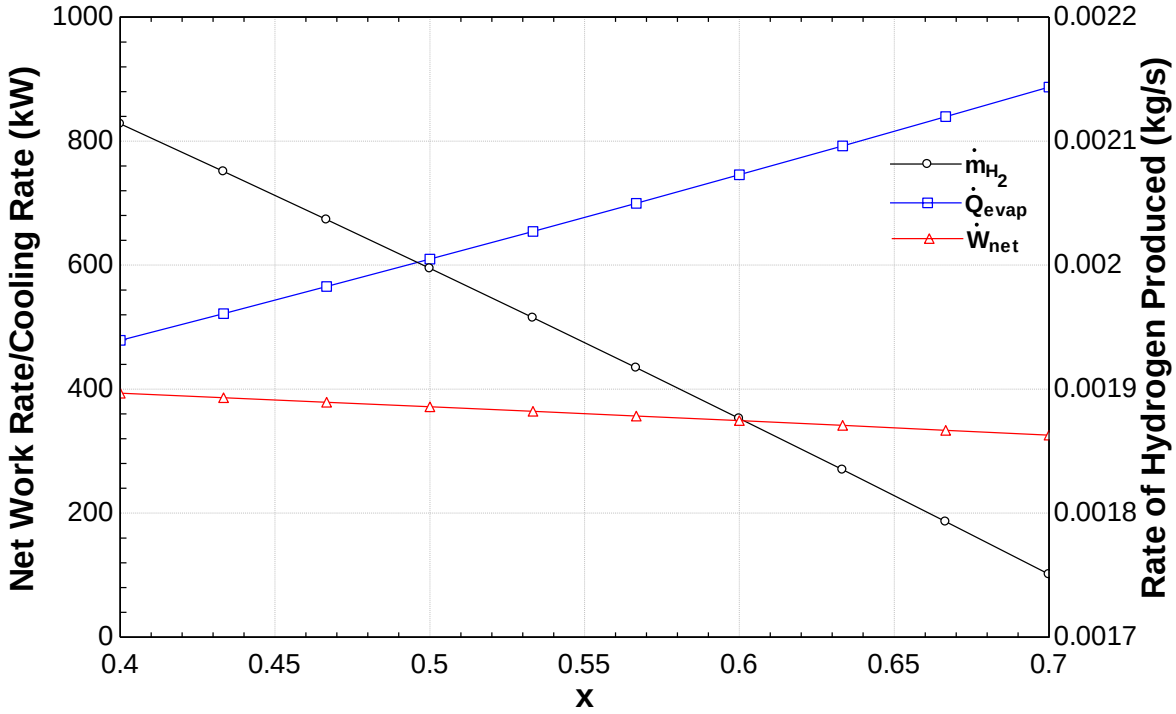

Figure 2.10 Variation of net work rate, cooling capacity and hydrogen produced with bleed ratio (x)

With the rise in work ratio from 0.1 to 0.9, the net work obtained by the overall system decreases; however, the rate of hydrogen produced rises. This somewhat explained by the fact that as the as the electricity in the electrolyzer rises, the rate of hydrogen generated rises resulting in the decrease in net work rate of the system. One should also note that work ratio does not have any effect on the cooling capacity of the system as it is run by the bleeding of the system which is not affecting with increase in work ratio (see Figure 2.9).

With the rise in bleed ratio from 0.4 to 0.7, the net work obtained by the system and mass of hydrogen production decreases. However, the quantity of cooling obtained increases. This due to the fact with the rise in bleed ratio, the heat input to the desorber2 increases causing cooling capacity to enhance (see Figure 2.10). However, with increase in bleed ratio, the amount of steam expands in the turbine decreases resulting in decreases in net work rate and hydrogen produced (see Figure 2.10). This trend is due to the fact that hydrogen produced and electrical work obtained are directly proportional to the amount of steam expanded in the turbine.

Chapter 3

Thermodynamic assessment of a new PTC operated polygeneration system for cooling, hydrogen production, fresh water, and electricity for a residential community

The current study aims to design a new parabolic trough collector (PTC) operated polygeneration system to produce freshwater, hydrogen, cooling, and electricity in a residential society. Dowtherm A (a heat transfer fluid) is used to transfer the heat from PTC to ORC, which is used to produce electrical power. The produced electrical power is utilized in three different ways, namely, to run the home appliances, to produce hydrogen (via water electrolysis), and to produce cooling (through a vapor compression cycle). The cooling produced by the vapor compression system is utilized to preserve the food, milk, and to operate the freezing desalination process. Effects of several factors, such as direct normal irradiance, evaporator temperature, and seawater inlet temperature, have been analyzed on the overall system behaviour. Thermodynamic study results show that for a PTC area of 2000 m^2, an electrical output obtained is 72 kW, the cooling rate is 112 kW, and the amount of fresh water generated is 18.4 l/day and 10.8 kg/day of hydrogen for mean solar irradiation of 700 W/m^2. The systems exergy efficiency is found to be 10.9% while its energy efficiency is 17.5%.

3.1 System Description

A polygeneration system utilizing sun energy via a parabolic trough collector (PTC) for producing freshwater, cooling, electricity, and hydrogen for a residential society is presented in Figure 3.1. The designed system has several components namely PTC, , condensers, evaporator, ORC turbine, compressor, electrolyzer, pumps, heat recovery vapor generator (HRVG), and throttle valve. PTC receives the solar radiation that is used to warm up the Dowtherm A (a heat transfer fluid) oil. The heated oil exits the PTC at state 1 and goes to HRVG. The oil exits HRVG at state 2 and is pushed back to PTC at state 3 via pump1. HRVG gains the heat by the heat transfer fluid and generates the vapor of R717 at state 4, which is being expanded to state 5 via the ORC turbine to produce mechanical power ($W_{t,,ORC}$). The expanded fluid coming at state 5 is condensed in condenser1 at state 6. The condensate at state 6, is pumped back to HRVG through pump2 at state 7. A fraction of electric power produced by the ORC turbine (W_{elec}) is used to run the proton exchange membrane (PEM) electrolyzer where water (at state 8) is being electrolyzed by electricity to produce hydrogen (at state 9) and oxygen (at state 10) via water splitting technology. The produced hydrogen is dispatched to the fuel station for fueling the vehicles (at state 22). Another fraction of electrical power produced by ORC turbine (W_{comp}) is to run the compressor of the vapor compression refrigeration (VCR) cycle. R134a is used as the

working fluid for VCR cycle due to its zero ozone depletion potential. Seawater or saline water enters the evaporator of the VCR cycle at state 16 and some portion of its changes to ice crystal by the cooling effect obtained in the evaporator. The rest of the seawater or saline water mainly in the form of brine leaves the evaporator at state 17. The ice crystals are being defreezed in the defreezing chamber, which is run by the heat produced in the condenser2 to produce freshwater, which is fed to the building for drinking purposes. The other part of cooling produced in the evaporator is used for cooling down the perishable food items (at state 23).

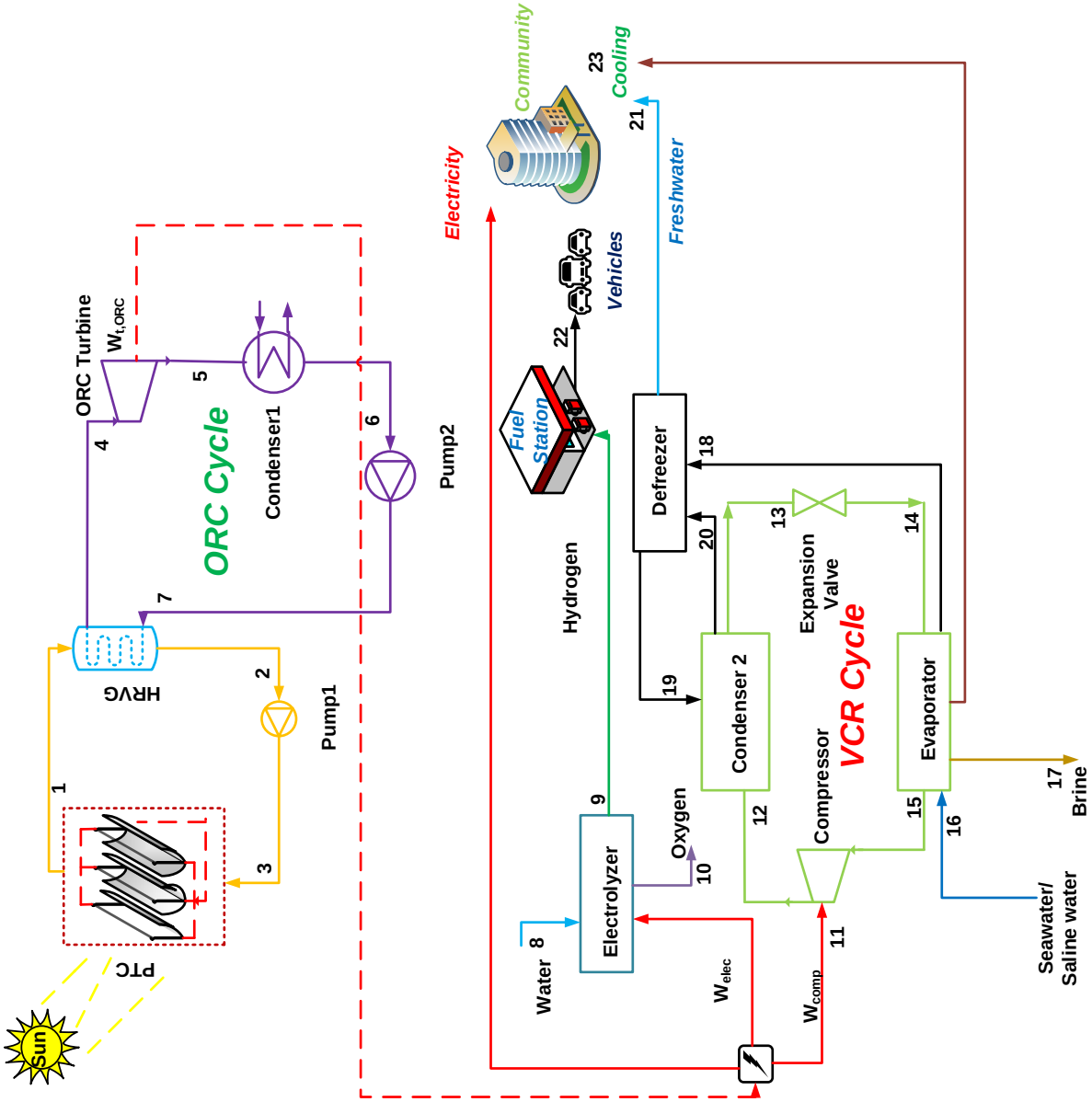

Figure 3.1 Schematic of a PTC based energy system for freshwater, cooling, hydrogen, and electricity

3.2 System Analyses

Thermodynamic assessment of the PTC-based energy system for freshwater, cooling, hydrogen, and electricity is presented in this section. Via exergy and energy analyses, the current system is checked for technical feasibility. To assist with the thermodynamic study several reasonable and conceptually correct assumptions have been considered namely as follows:

- The rate of heat loss in all the heat exchangers has been neglected.
- An analysis is performed when system parameters do not vary with time.
- Pressure drops across the pipelines are neglected.
- An average solar sunshine hour is assumed as seven.
- No chemical exergy is considered except in the electrolyzer.
- No heat is being loss in the turbine, compressor and pumps.

We have analyzed our system thermodynamically by balance equations for each unit used in the system. The rate of energy and exergy for key element of the designed system are arranged in Table 3.1.

Table 3.1 Exergy and energy balance rate of the key elements of the system

Element	Energy balance equation	Exergy balance equation
PTC	$\dot{m}_3 h_3 + \dot{Q}_{sol} = \dot{m}_1 h_1 + \dot{Q}_{loss,PTC}$	$\dot{m}_3 ex_3 + \dot{E}x_{sol}^{Q} = \dot{m}_1 ex_1 + \dot{Q}_{loss,PTC}\left(1 - \frac{T_0}{T_1}\right) + \dot{E}x_{d,PTC}$
HRVG	$\dot{m}_1 h_1 + \dot{m}_7 h_7 = \dot{m}_4 h_4 + \dot{m}_2 h_2$	$\dot{m}_1 ex_1 + \dot{m}_7 ex_7 = \dot{m}_4 ex_4 + \dot{m}_2 ex_2 + \dot{E}x_{d,HRVG}$
ORC Turbine	$\dot{m}_4 h_4 = \dot{m}_5 h_5 + \dot{W}_{t,ORC}$	$\dot{m}_4 ex_4 = \dot{m}_5 ex_5 + \dot{W}_{t,ORC} + \dot{E}x_{d,t,ORC}$
Compressor	$\dot{m}_{15} h_{15} + \dot{W}_{comp} = \dot{m}_{12} h_{12}$	$\dot{m}_{15} ex_{15} + \dot{W}_{comp} = \dot{m}_{12} ex_{12} + \dot{E}x_{d,comp}$
Evaporator	$\dot{m}_{14} h_{14} + \dot{Q}_{cooling} + \dot{m}_{16} h_{16} = \dot{m}_{15} h_{15} + \dot{m}_{17} h_{17} + \dot{m}_{18} h_{18}$	$\dot{m}_{14} ex_{14} + \dot{Q}_{cooling}\left(\frac{T_0}{Tevap} - 1\right) + \dot{m}_{16} ex_{16} = \dot{m}_{15} ex_{15} + \dot{m}_{17} ex_{17} + \dot{m}_{18} ex_{18} + \dot{E}x_{d.evap}$

Electrolyzer	$\dot{m}_8 h_8 + \dot{W}_{elec} = \dot{m}_9 h_9 + \dot{m}_{10} h_{10} + \dot{Q}_{loss,elec}$	$\dot{m}_8 ex_8 + \dot{W}_{elec} = \dot{m}_9 ex_9 + \dot{m}_{10} ex_{10} + \dot{Q}_{loss,elec}\left(1 - \frac{T_0}{T_{elec}}\right) + \dot{E}x_{d,elec}$
Throttle Valve	$\dot{m}_{13} h_{13} = \dot{m}_{14} h_{14}$	$\dot{m}_{13} ex_{13} = \dot{m}_{14} ex_{14} + \dot{E}x_{d,tv}$
Defreezer	$\dot{m}_{18} h_{18} + \dot{m}_{20} h_{20} = \dot{m}_{19} h_{19} + \dot{m}_{21} h_{21}$	$\dot{m}_{18} ex_{18} + \dot{m}_{20} ex_{20} = \dot{m}_{19} ex_{19} + \dot{m}_{21} ex_{21} + \dot{E}x_{d,defreezer}$

After writing the balance equations for all the component used in the present system, we analyze solar parabolic trough collector and other component with the establish equations in the literature.

Solar Parabolic Trough Collector Analysis

For solar parabolic trough collector analysis, determination of thermal efficiency of the collector is vital as it is highly affected by the solar irradiation received.

To evaluate the thermal efficiency of the PTC, the following expression is used [69]

$$\eta_{th,PTC} = 0.75K(\theta) - 0.000045(T_3 - T_0) - 0.039\left(\frac{T_3 - T_0}{DNI}\right) - 0.3\left(\frac{T_3 - T_0}{DNI}\right)^2 \quad (3.1)$$

where DNI is the direct normal solar irradiation and T_0 represents the environment temperature.

Freezing Process

To evaluate the performance of the freezing desalination process, the following methodology is adopted [41].

The rate of formation of ice is given as

$$\dot{m}_{ice} = \dot{m}_{sw} IR \quad (3.2)$$

where $\dot{m}_{sw}$ is the rate of mass of seawater.

The ice ratio (IR) is determined as

$$IR = \frac{X_f(1-C)}{X_d - CX_f} \quad (3.3)$$

where C represents the concentration ratio, salinity of feed water is depicted by X_f and X_d shows the freshwater salinity.

The concentration ratio (C) is depicted as $C = \frac{X_b}{X_f}$.

Feedwater salinity in ppm, X_f can be computed as

$$X_f = Salinity \times 10^6 \quad (3.4)$$

Brine salinity, X_b can be found as

$$X_f = \frac{X_f \dot{m}_{sw} - \dot{m}_{ice} X_d}{\dot{m}_b} \quad (3.5)$$

The flow rate of brine flow rate is calculated as

$$\dot{m}_b = \dot{m}_{sw}(1 - IR) \quad (3.6)$$

The freezing point of the seawater, $T_{freezing}$ (°C) is calculated as [70]

$$T_{freezing} = -0.5369 Salinity - 0.0172 \qquad for\ 0.5\% \leq Salinity \leq 4\% \quad (3.7)$$

Overall System

Systems' exergy and energy efficiencies are used to get the systems' performance. One uses the following relation to evaluate the systems' energy efficiency:

$$\eta_{en,ov} = \frac{(\dot{Q}_{cooling} + \dot{En}_{out,water} - \dot{En}_{in,sw} + \dot{W}_{net} + \dot{m}_{H2} LHV)}{\dot{Q}_{sol}} \quad (3.8)$$

where $\dot{m}_{H,2}$ represents the amount of hydrogen produced and $\dot{Q}_{cooling}$ shows amount of cooling obtained by the system and $\dot{W}_{net}$ shows the rate of net work produced through the system. $\dot{En}_{out,water} - \dot{En}_{in,sw}$ can are the energy content of the outlet water and seawater, respectively. The details can be found elsewhere [41].

Similarly, the systems' exergy efficiency is evaluated as

$$\eta_{ex,ov} = \frac{(\dot{Ex}^Q_{cooling} + \dot{Ex}_{out,water} - \dot{Ex}_{in,sw} + \dot{W}_{net} + \dot{m}_{H2} ex_{H2})}{\dot{Ex}^Q_{sol}} \quad (3.9)$$

where $\dot{Ex}^Q_{cooling} = \dot{Q}_{cooling}\left(\frac{T_0+273}{Tevap+273} - 1\right)$ and $\dot{Ex}^Q_{sol}$ represents the thermal exergy of solar irradiation.

3.3 Results and Discussion

On a typical summer day, in India (environment temperature of 35°C, direct normal irradiation of 0.7 kW/m^2), the presented system will give electrical power to a housing society of around 60 houses/apartment (having 250 people) in a sustainable way. Furthermore, the proposed system could be able to deliver a cooling load of 2 kW per house. With the designed system, hydrogen generated would be sufficient to power 50 vehicles for an average driving range of 80 km. Key

parameters applied in the present analysis are listed in Table 3.2. The outlet temperature of PTC is 247.6℃ and area is 2000 m^2. Our results match closely with the results of other researchers. For instance, energy efficiency of the PTC used in our system comes out to be 70.1% which matches closely with the value reported by Tzivanidis et al. [71].

Table 3.2 Parameter used for the system analysis

State Point	**Type of Fluid**	**Temperature (^oC)**	**Pressure (kPa)**	**ṁ (kg/s)**	**h (kJ/kg)**	**s (kJ/kgK)**	**ex (kJ/kg)**
1	Dowtherm A	247.6	101	11.55	551.2	1.076	191.0
2	Dowtherm A	217.6	101	11.55	465.4	0.9432	144.9
3	Dowtherm A	218	101	11.55	465.4	0.9432	145.01
4	R717	244.6	16000	0.693	1826.0	5.063	738.7
5	R717	36.3	1400	0.693	1448	5.063	360.3
6	R717	36.3	1400	0.693	372.1	1.586	320.7
7	R717	40.4	16000	0.693	396.9	1.586	345.4
8	Water	25	101	0.00386	104.8	0.3672	0
9	Hydrogen	25	101	0.000429	142000	53.39	134900
10	Oxygen	25	101	0.0034	0.0	0.00	0
11	-	-	-				
12	R134a	70	1200	1.67	300.6	0.9938	57.43
13	R134a	44.7	1150	1.67	115.3	0.4167	44.08
14	R134a	-8.9	210	1.67	115.3	0.4452	35.56
15	R134a	-5	200	1.67	248.8	0.9541	17.47
16	Seawater/Saline	25	101	0.00183	-	-	0.1919

	water						
17	Brine	25	101	0.0011	-	-	5.004
18	Ice crystal	-0.2857	101	0.00073	-	-	2.62
19	-	-	-				
20	-	-	-				
21	Water	25	101	0.00073	-	-	0.00

Source: [65,69]

Table 3.3 Values of various factors obtained in the present work

Parameter	**Value**
Rate of net electric work produced (kW)	72.0
Work rate consumed by the electrolyzer (kW)	86.6
Work rate consumed by the compressor (kW)	86.6
Rate of Cooling (kW)	112.0
Systems' energy efficiency (%)	17.5
Systems' exergy efficiency (%)	10.9
Evaporator temperature (°C)	-5
Rate of hydrogen produced (kg/day)	10.8
Compressors' isentropic efficiency (%)	74.1
Electrolyzers' energy efficiency (%)	70.0
Electrolyzers' exergy efficiency (%)	66.8

The numerical values of several key variables found from the thermodynamic assessment of the presented system are given in Table 3.3. One can see that for a PTC area of 2000 m^2, the rate of network generated by the system is 72.0 kW with a rate of cooling capacity of 112 kW. Analysis shows that the exergy efficiency of the electrolyzer used in the study is 66.8%. The electrolyzer used in the study can generate 0.0004288 kg/s of hydrogen. Furthermore, the isentropic efficiency of the compressor of the vapor compression cycle is found to be 74.1%.

The following methodology as depicted in flow chart (Figure 3.2) is being followed.

- Mathematical model for the proposed and developed systems are done and full thermodynamic balance equations for the overall systems and components like electrolyser, heat exchangers, solar collectors etc are written.
- Energy and exergy balance rate equations for each element by writing a program in the software named as an engineering equation solver (EES).
- Determination of exergy destruction rate and exergy efficiency of each component of the developed energy systems is done.
- Performance assessment of the developed systems via energy and exergy efficiencies.
- Parametric study of each system individually to see the impact of design factors on the systems performance.

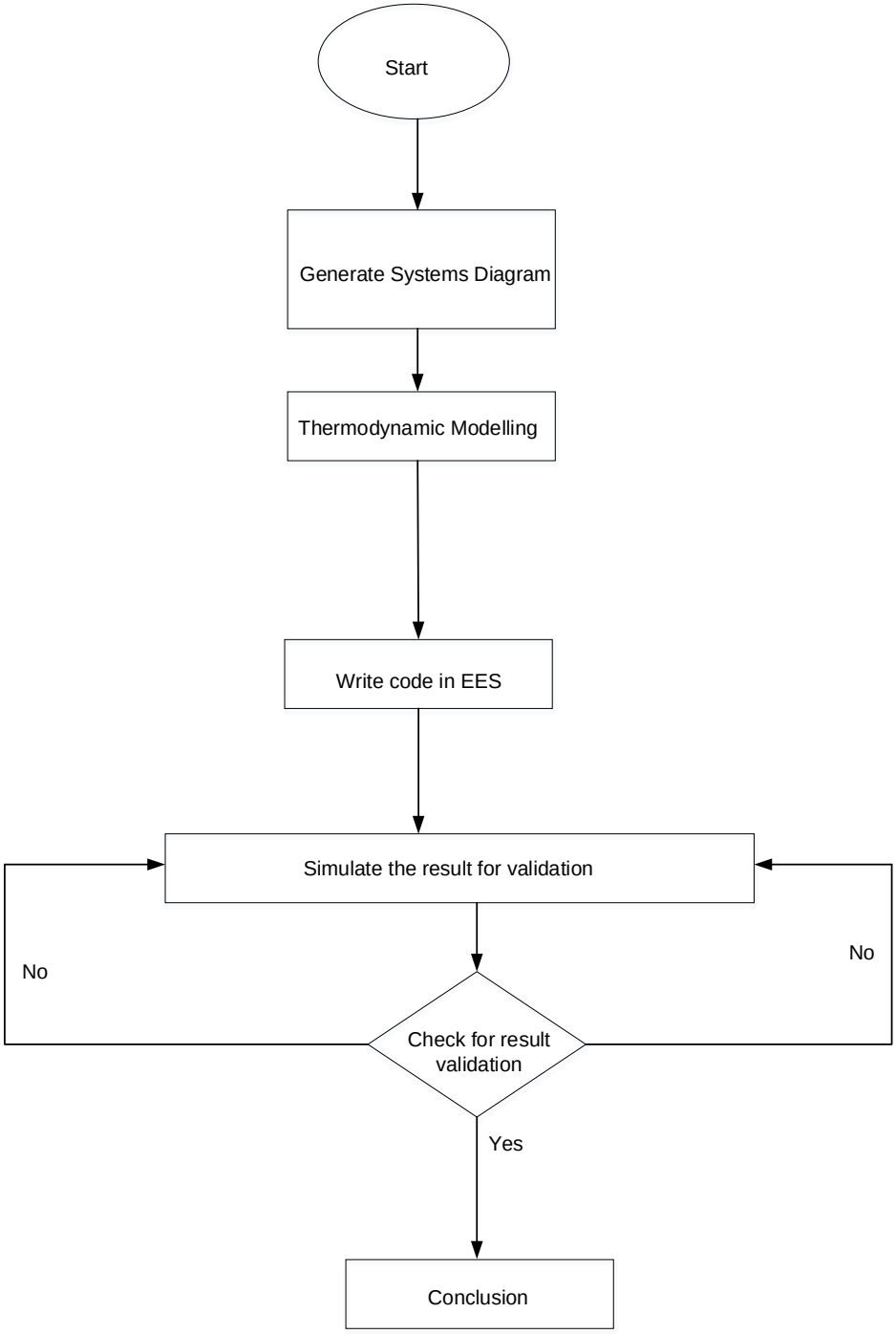

Figure 3.2 Flow chart used in the analysis with procedure and method

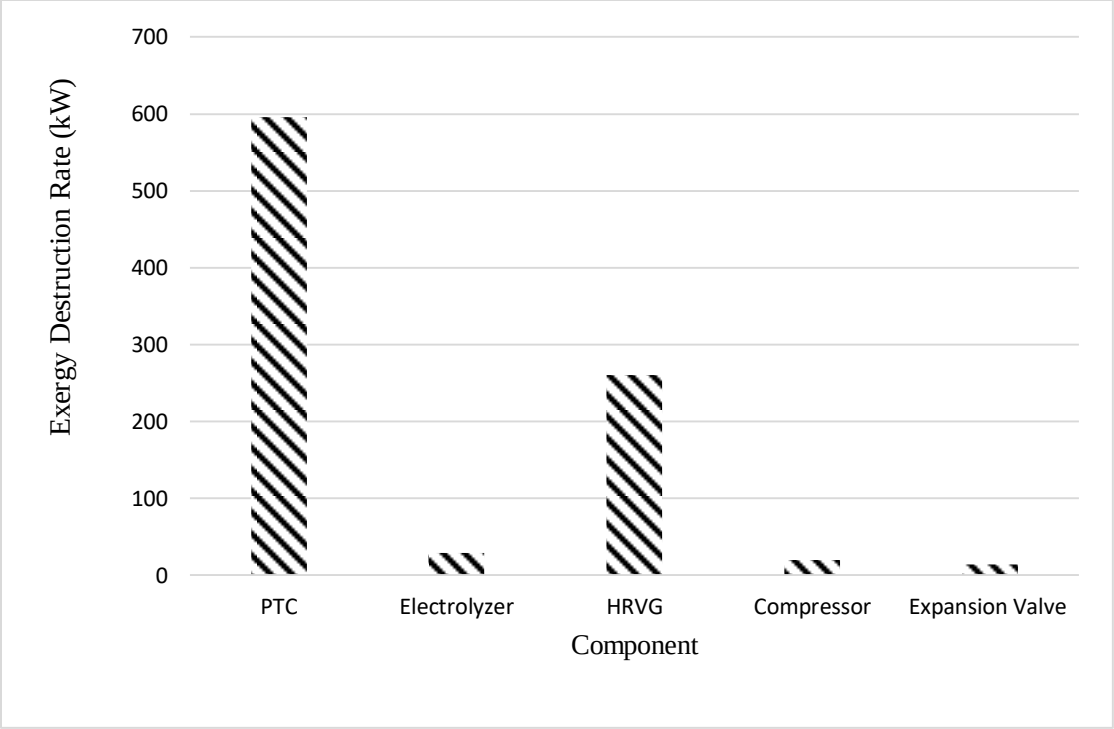

Figure 3.3 Exergy destruction rate of various element used in the present system

The exergy destruction rate for the various elements used in the present system are calculated and displayed in Figure 3.3. For the presented system, 596 kW of exergy is being destroyed in the parabolic trough collector followed by heat recovery vapor generator i.e. 260 kW. Highest rate of exergy destruction happens in the PTC because of entropy being destroyed by the large heat losses across the PTC. The exergy destruction rate in the electrolyzer is significant as their electricity is being utilized to produce hydrogen i.e. high grade of energy is being used to produce the fuel.

Figure 3.4 shows the variation in systems' energy and exergy efficiencies with ORC turbine inlet pressure. With the rise in pressure from 10 MPa to 30 MPa, the systems' efficiency (changes from 15.6% to 18.3%) rises. However, the systems' exergy efficiency increases and reaches a extreme at around 21.500 MPa and then decreases. This result shows that the optimum pressure to operate the system is around 21.500 MPa from exergetic point of view at a given inlet temperature of the ORC turbine for a chosen fluid (R717).

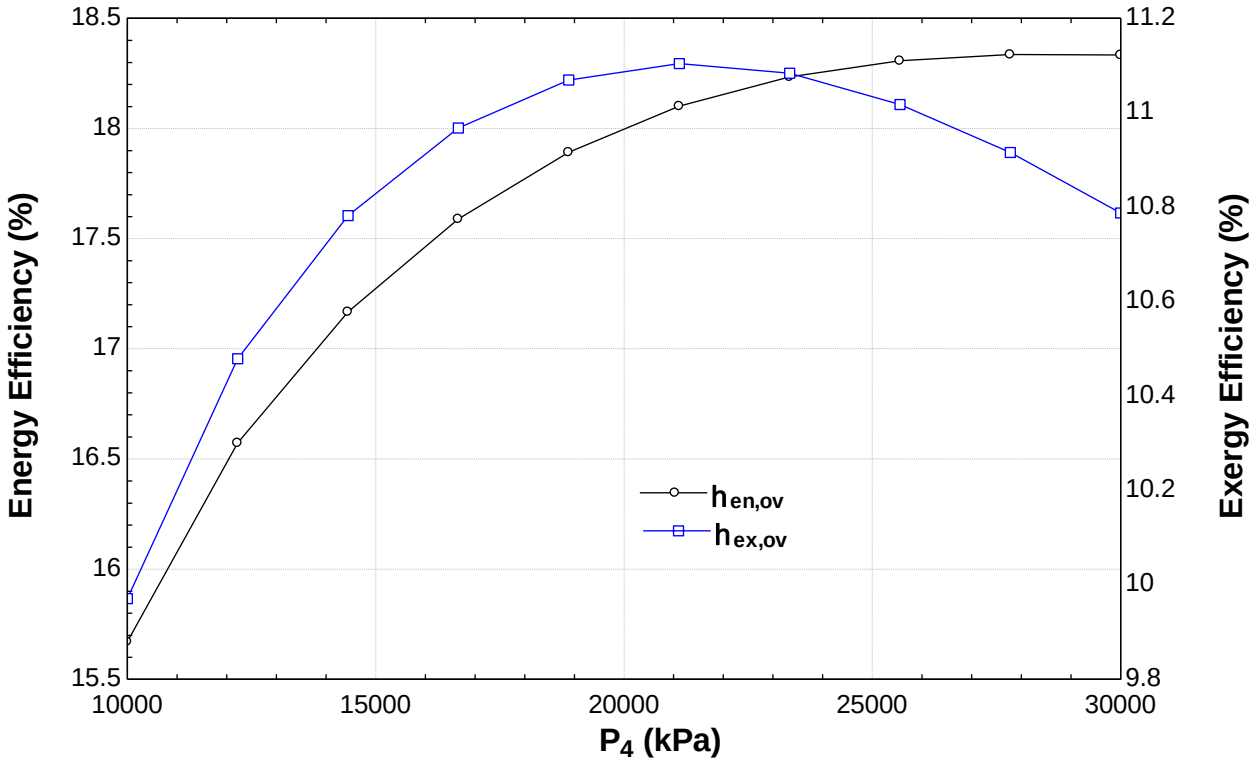

Figure 3.4 Changes of systems' exergy and energy efficiencies with ORC turbine inlet pressure

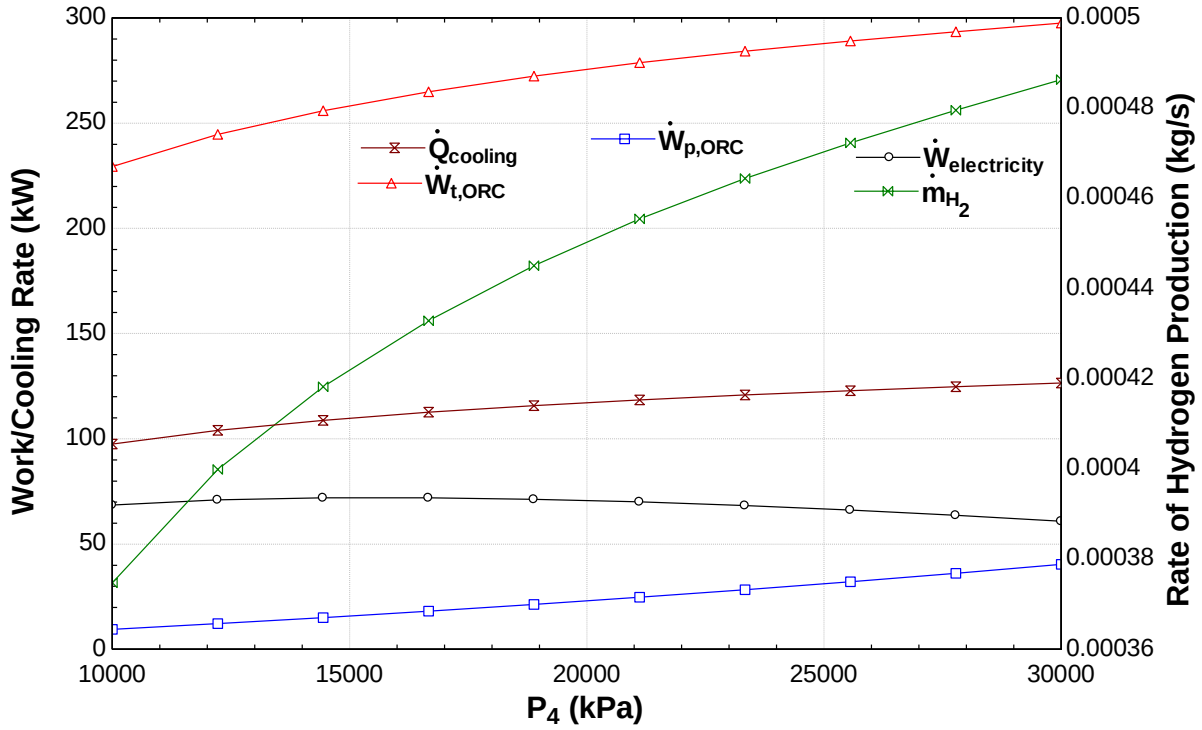

Figure 3.5 Variation of electrical work, ORC pump work, ORC turbine work, rate of hydrogen production, and cooling with ORC turbine inlet pressure

Figure 3.5 demonstrates the change of electricity, ORC pump work, ORC turbine work, rate of hydrogen production, and cooling with the inlet pressure of ORC turbine. With the rise in pressure from 10,000 kPa to 30,000 kPa, the network rate increases first rise from 68.5 kW to 70.0 kW and then starts decreasing to 60.8 kW while the rate of cooling capacity improves from 97.5 kW to 126.5 kW. The rate of hydrogen produced also rises with the change in pressure i.e., 0.000375 kg/s to 0.000486 kg/s.

Result of temperature difference (T_1-T_4) on the systems' exergy and energy efficiencies are drawn in Figure 3.6. As the temperature difference rises from 2℃ to 10℃, there is a slight decline in both the efficiencies. This trend is because as the temperature difference rises, there is a decline in the inlet temperature of the ORC turbine which causes a decline in ORC turbine work rate leading to exergy and energy efficiencies of the system fall.

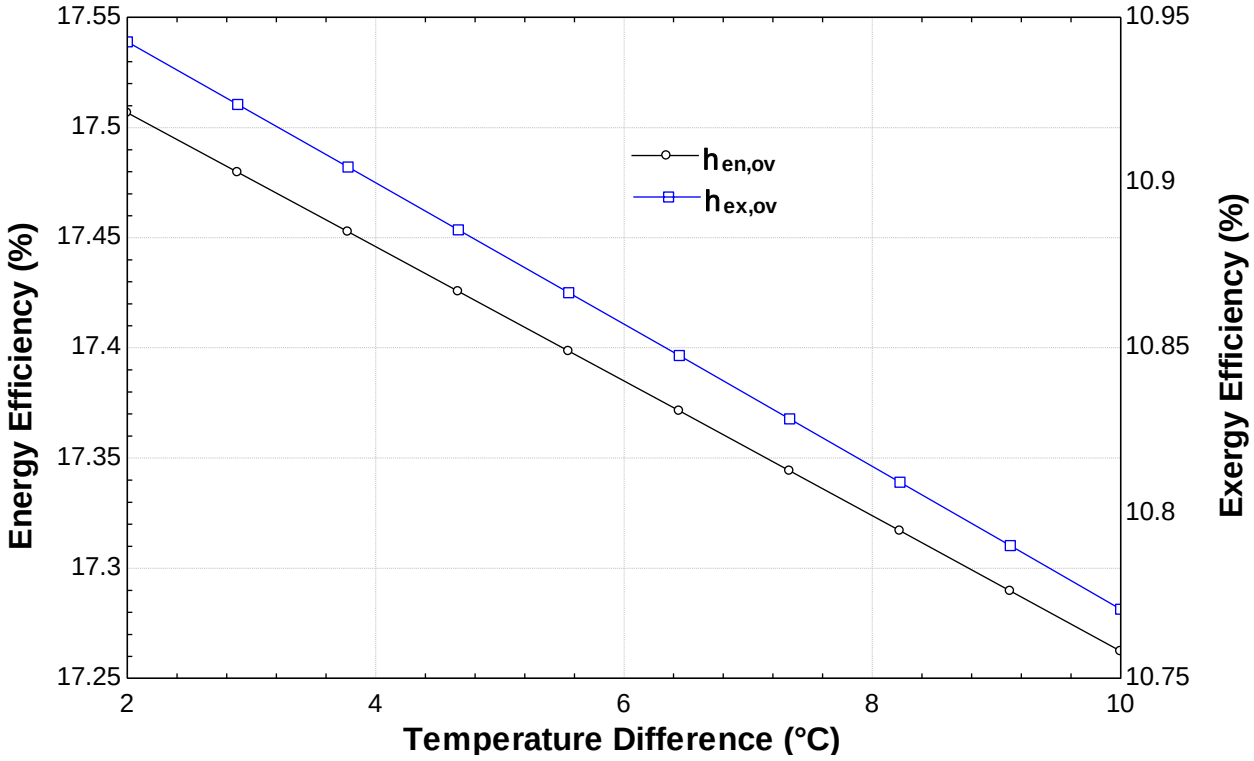

Figure 3.6 Result of temperature difference on the systems' exergy and energy efficiencies

With the rise in temperature difference from 2℃ to 10℃, a slight decline in all the considered parameters (electrical work, compressor work, ORC turbine work, and rate of cooling) is observed (see Figure 3.7). This is because as the temperature difference rises, the net thermal energy available to the ORC cycle decreases leading to a slight decrease in all the parameters.

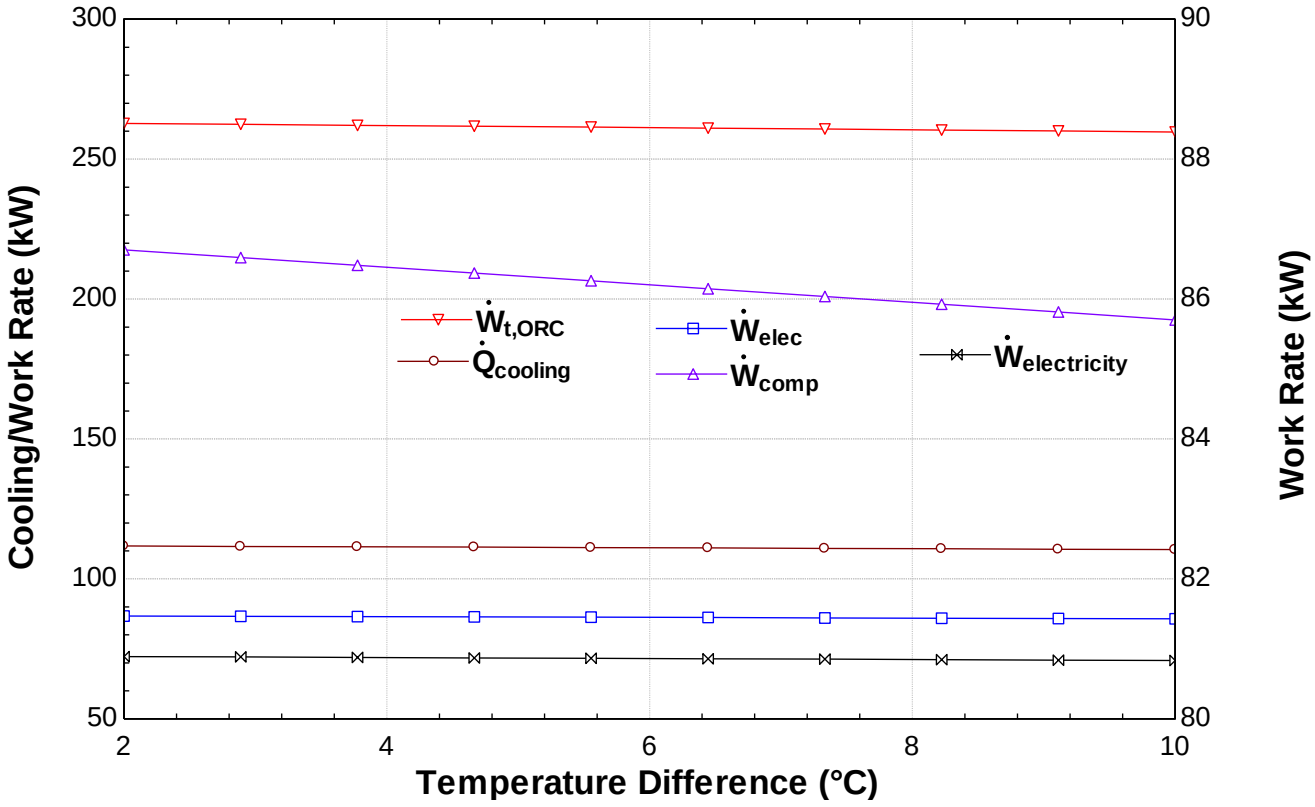

Figure 3.7 Result of temperature difference on the electrical work, compressor work, ORC turbine work, and rate of cooling

The variation of direct normal irradiation (DNI) on the systems' exergy and energy efficiencies and parabolic trough collector is plotted in Figure 3.8. With the change in irradiation changes from 200 W/m^2 to 1000 W/m^2, the energy efficiencies of both PTC and the overall system change drastically. A similar trend is observed for the systems' and PTCs' exergy efficiencies. From figure one can note that the efficiency of PTC has a key role in the behavior of the overall system. Thus, attempts should be done to improve the efficiency of PTC. These efforts need to be cost effective as well.

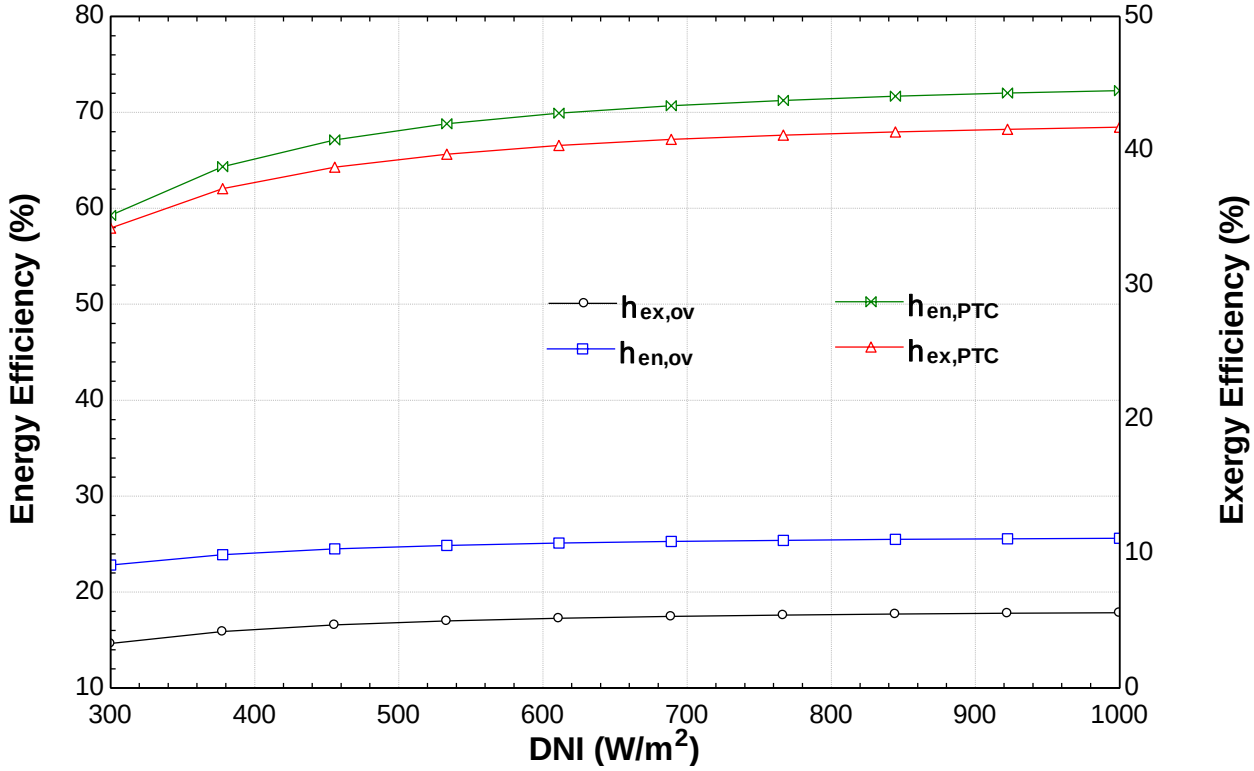

Figure 3.8 Result of solar irradiance on the PTCs' and systems' exergy and energy efficiencies

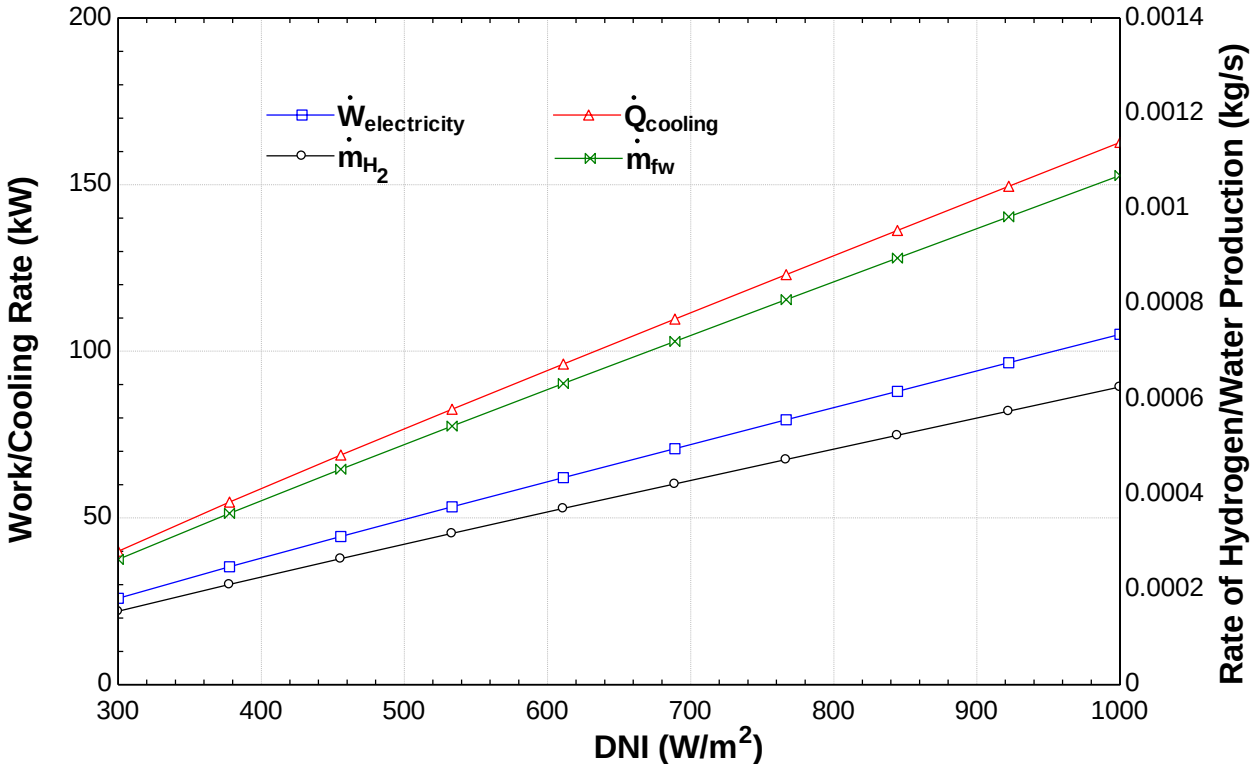

Figure 3.9 Result of solar irradiance on the electrical work, rate of cooling, hydrogen, and freshwater production

As the direct normal irradiation rises, the rate of hydrogen production, electrical work, rate of freshwater, and cooling all increase significantly (see Figure 3.9). This trend is because with the increase in DNI, the output temperature of the PTC increases, resulting in higher turbine inlet temperature of ORC, leading to higher ORC turbine output, causing all the useful outputs of the system to enhance.

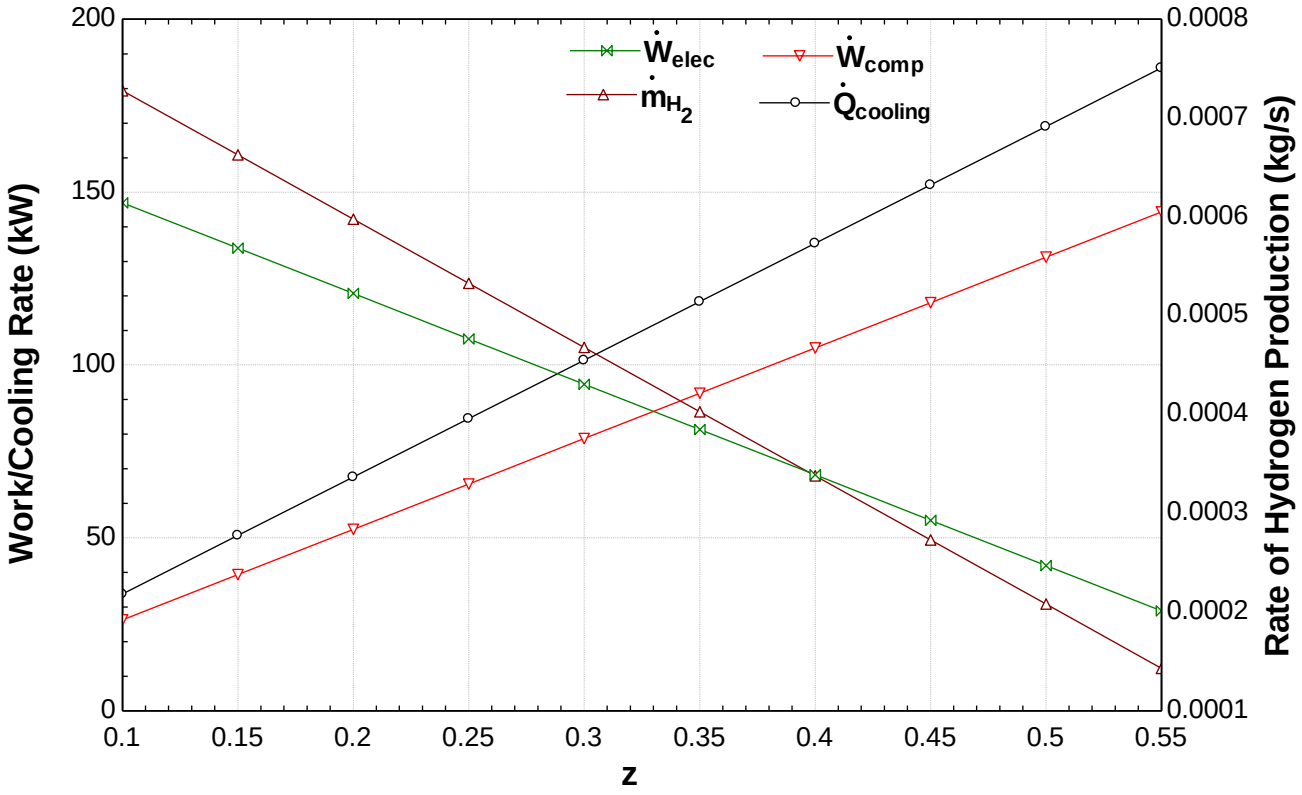

Figure 3.10 Influence of cooling to power ratio (z) on the network rate, compressor work, rate of cooling, and hydrogen production

It is noticed from the Figure 3.10, that as the ratio (z) increases, the work done by the compressor of the vapor compression cycle rises as well as the cooling rate of the system improves while the rate of hydrogen production and net electricity produced by the system decreases. Figure 3.11 shows the effect of cooling to power ratio (z) on the performance of the system i.e. energy and exergy efficiencies of the system. As the cooling to power ratio increases from 0.1 to 0.55, the

energy efficiency considerably rises from 15.0% to 20.0%. This rise can be attributed to the fact that more cooling can be achieved via the vapor compression cycle due to its higher COP (mostly greater than unity). Furthermore, it is to be noted from the figure that the exergy efficiency of the system declines with the rise in the ratio (z). This trend is observed due to the fact the exergetic output of the cooling is lower than the used electricity in the compressor of the vapor compression cycle.

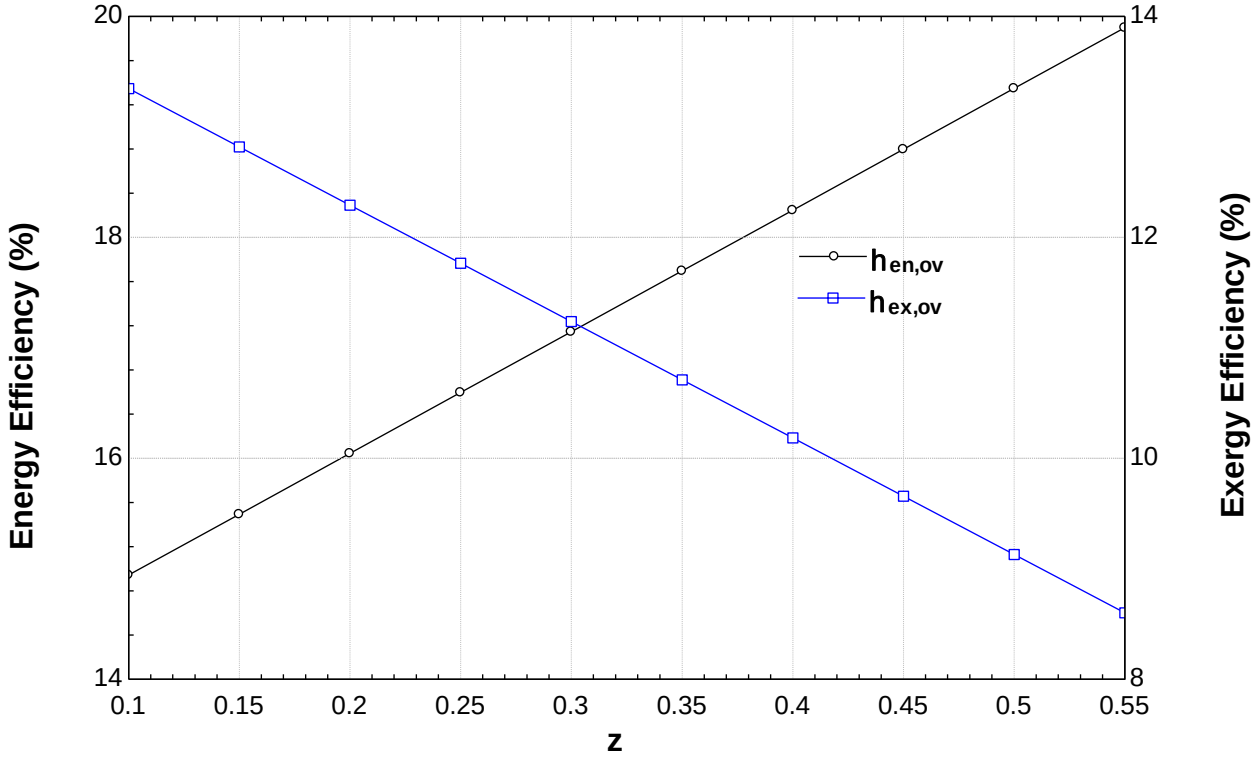

Figure 3.11 Exergy and energy efficiencies of the system variation with the cooling to power ratio (z)

The effect of freshwater to evaporator cooling ratio (a) on the cooling rate and amount of hydrogen generated is plotted in Figure 3.12. As the ratio (a) increases from 0.3 to 0.75, the cooling rate decreases from 156.2 kW to 55.8 kW and the amount of freshwater obtained rises from 10.8 kg/day to 27.7 kg/day. This is obvious from the fact that as the amount of freshwater increases, the demand for freezing rises resulting in the overall decrease in cooling rate. It is to be noted further from Figure 3.13 that as the ratio (a) rises, the exergetic and energetic performance of the system reduce. This trend is somewhat explained by the point that the energetic and exergetic content of freshwater is way less compared to that of cooling.

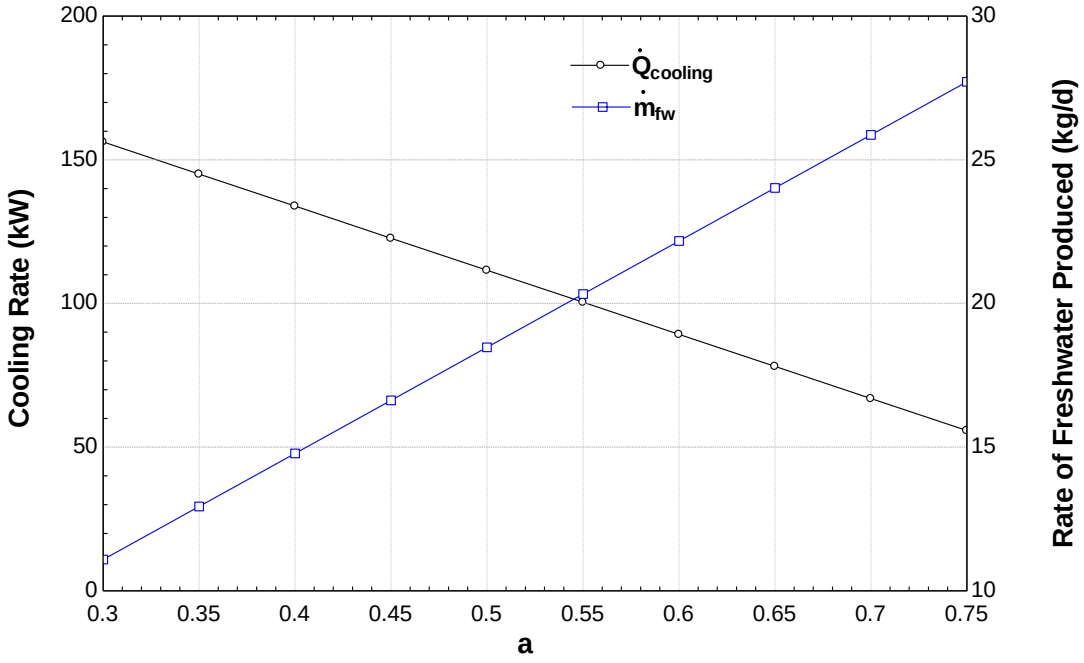

Figure 3.12 Effect of freshwater to evaporator cooling ratio (a) on the rate of cooling, and hydrogen production

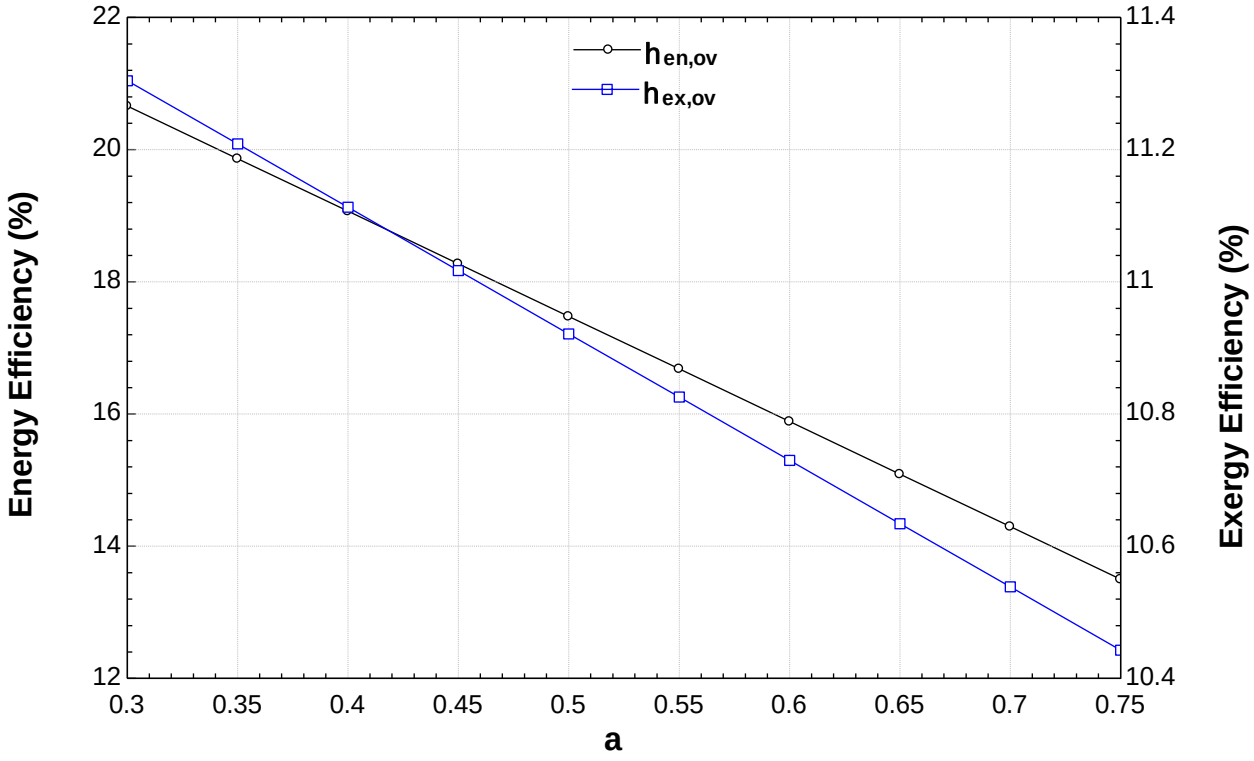

Figure 3.13 Variation of systems' exergy and energy efficiencies with freshwater to evaporator ratio (a)

Chapter 4

Feasibility study of a new solar based trigeneration system for fresh water, cooling and electricity production

Utilization of solar energy to generate electricity, cooling, and freshwater in remote areas in a sustainable way still poses lots of challenges to the researchers. The goal of the current work is to design a new solar-operated trigeneration system to produce electricity, cooling and fresh water using parabolic trough collectors in remote areas. Electric power is generated by using Organic Rankine Cycle, and cooling and fresh water (using freezing desalination technique) is obtained by two-stage NH_3-H_2O vapor absorption system run by solar energy. Simulation results show that for PTC arrays of 200 m^2, an electrical output obtained is 3.3 kW, cooling rate is 20.4 kW, and mass flow rate of freshwater produced is 36 kg/h for an average solar irradiance of 700 W/m^2. Additionally, sensitivity analysis is conducted by varying the parameter like solar irradiation, evaporator temperature, seawater inlet temperature etc. and their effect on performance characteristics of the overall setup is investigated.

4.1. System Description

The proposed solar operated trigeneration system using parabolic trough collector consists of ORC, two-stage absorption refrigeration system (NH_3-H_2O based) with precooling, and freeze water desalination system to produce electrical power, cooling, and freshwater (Figure 4.1). This trigeneration is branched into four subsystems. Subsystem-I (HTF cycle), Subsystem-II (ORC), Subsystem-III (two-stage vapor absorption refrigeration cycle), and Subsystem-IV (freeze desalination cycle). Dowtherm A (a heat transfer fluid) goes to the PTC at state 33 where its temperature is increased by capturing the radiation from sun. Hot HTF at state 30 coming out from PTC enters the HRVG of ORC to vaporize the refrigerant (R290) at state 34 and this vaporised refrigerant enters the turbine and power produces. The turbine exits at state 35 through condenser and pump enters to HRVG at state 37 to complete the ORC. After vaporizing the refrigerant, HTF at state 31 passes through desorber-2 of the two-stage absorption system and leaves at 32 to enter the pump and then in the PTC field at state 33 to complete the HTF cycle. Two stage vapor absorption system consists of state point from 1 to 29. Salient features of this two -stage system is: the desorber -2, which receives the heat from HTF; the desorber-1, which receives the heat from rectifier-2 (Rect2) & absorber-2; heat lost by rectifiers (Rect1 & Rect3) & absorber-1 is thrown to the environment. Refrigerant in the evaporator of two -stage system performs two functions: first is to separate the sea water (at state 38) into ice-crystal at state 42 & brine at state 39 by absorbing the heat from sea water; and second is to provide space cooling.

Ice crystals formed in evaporator is taken to the defreezer then converted into fresh water at state 43 by the heat rejected by condenser-2 and then it is collected in the tank.

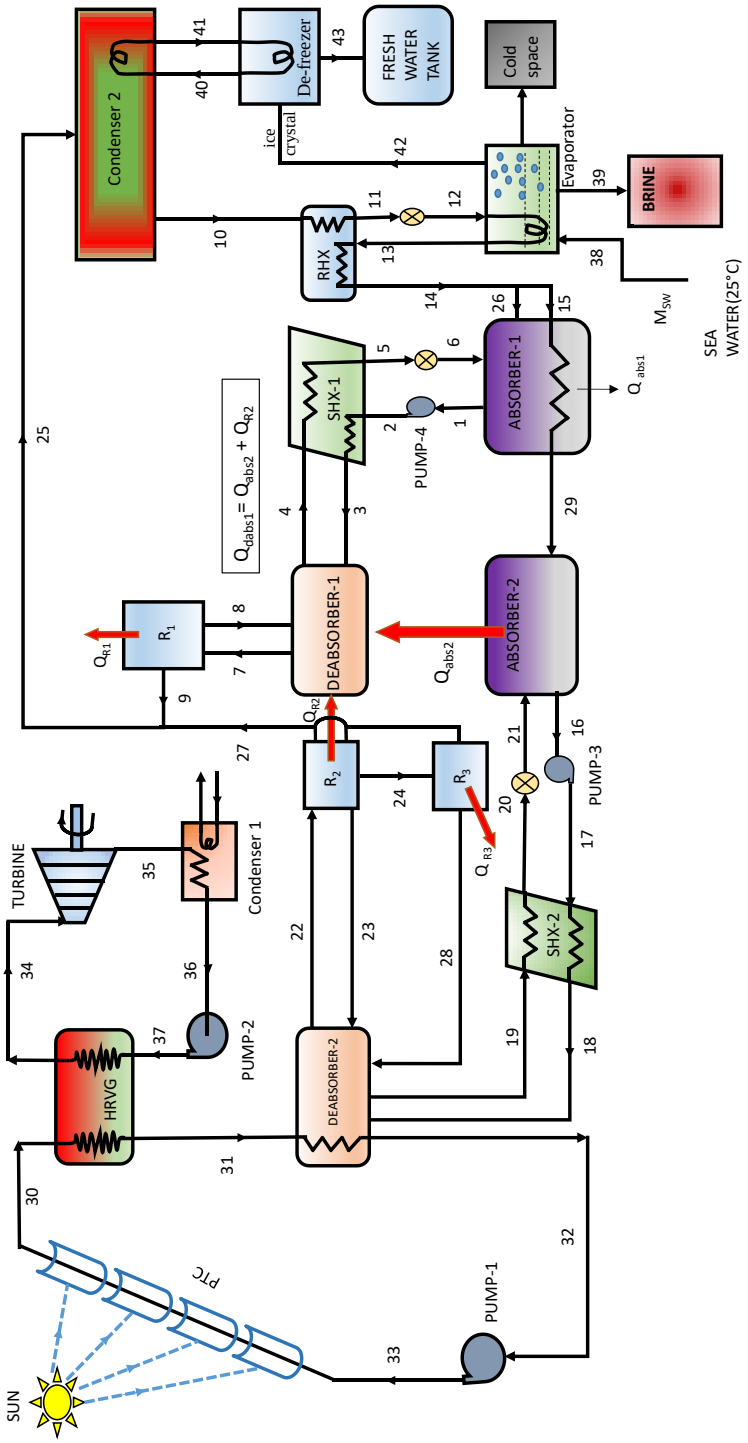

Figure 4.1 Sketch of a new solar driven trigeneration system for electrical power, cooling, and freshwater

4.2 System Analyses

The trigeneration system presented in section 4.2 is evaluated by thermodynamic principles using energy and exergy analyses for technical feasibility. Various reasonable and conceptually correct assumptions are invoked to ease the analysis which are as follows:

- The loss of pressure in the pipelines of heat exchanger, and other devices are negligible.
- All the turbine, pumps and compressor operate in adiabatic state.
- System operates in the steady state.

Table 4.1 lists the exergy and energy balance rate for the key component of the system in section 4.2.

Table 4.1 Exergy and energy balance rate for the key component of the system used in the current study

Component	Energy equation	Exergy equation
PTC	$\dot{m}_{33}h_{33} + \dot{Q}_{sol} = \dot{m}_{30}h_{30} + \dot{Q}_{loss,PTC}$	$\dot{m}_{33}ex_{33} + \dot{E}x_{sol}^{Q} = \dot{m}_{30}ex_{30} + \dot{Q}_{loss,PTC}\left(1 - \frac{T_0}{T_{30}}\right) + \dot{E}x_{d,PTC}$
HRVG	$\dot{m}_{30}h_{30} + \dot{m}_{37}h_{37} = +\dot{m}_{34}h_{34} + \dot{m}_{31}h_{31}$	$\dot{m}_{30}ex_{30} + \dot{m}_{37}ex_{37} = \dot{m}_{34}ex_{34} + \dot{m}_{31}ex_{31} + \dot{E}x_{d,HRVG}$
Condenser 2	$\dot{m}_{35}h_{35} = \dot{m}_{36}h_{36} + \dot{Q}_{cond2}$	$\dot{m}_{35}ex_{35} = \dot{m}_{36}ex_{36} + \dot{Q}_{cond2}\left(1 - \frac{T_0}{T_{36}}\right) + \dot{E}x_{d,cond2}$
Desorber 2	$\dot{m}_{23}h_{23} + \dot{m}_{18}h_{18} + \dot{m}_{28}h_{28} + \dot{m}_{31}h_{31} = \dot{m}_{19}h_{19} + \dot{m}_{22}h_{22} + \dot{m}_{32}h_{32}$	$\dot{m}_{23}ex_{23} + \dot{m}_{18}ex_{18} + \dot{m}_{28}ex_{28} + \dot{m}_{31}ex_{31} = \dot{m}_{19}ex_{19} + \dot{m}_{22}ex_{22} + \dot{m}_{32}ex_{32} + \dot{E}x_{d,desorb2}$
Desorber 1	$\dot{m}_3h_3 + \dot{m}_8h_8 + \dot{Q}_{abs2} + \dot{Q}_{rect2} = \dot{m}_7h_7 + \dot{m}_4h_4$	$\dot{m}_3ex_3 + \dot{m}_8ex_8 + \dot{Q}_{abs2}\left(1 - \frac{T_0}{T_{16}}\right) + \dot{Q}_{rect2}\left(1 - \frac{T_0}{T_{24}}\right) = \dot{m}_7ex_7 + \dot{m}_4ex_4 + +\dot{E}x_{d,desorb1}$
Rectifier 2	$\dot{m}_{22}h_{22} = \dot{m}_{23}h_{23} + \dot{m}_{24}h_{24} + \dot{Q}_{rect2}$	$\dot{m}_{22}ex_{22} = \dot{m}_{23}ex_{23} + \dot{m}_{24}ex_{24} + \dot{Q}_{rect2}\left(1 - \frac{T_0}{T_{24}}\right) + \dot{E}x_{d,rect2}$

Evaporator	$\dot{m}_{12}h_{12} + \dot{Q}_{cooling} + \dot{m}_{38}h_{38} = \dot{m}_{39}h_{39} + \dot{m}_{13}h_{13} + \dot{m}_{42}h_{42}$	$\dot{m}_{12}ex_{12} + \dot{Q}_{cooling}\left(1 - \frac{T_0}{Tevap}\right) + \dot{m}_{38}ex_{38} = \dot{m}_{39}ex_{39} + \dot{m}_{13}ex_{13} + \dot{m}_{42}ex_{42} + \dot{E}x_{d.evap}$
Absorber 1	$\dot{m}_{15}h_{15} + \dot{m}_6h_6 + \dot{m}_{26}h_{26} = \dot{m}_1h_1 + \dot{m}_{29}h_{29} + \dot{Q}_{abs1}$	$\dot{m}_{15}ex_{15} + \dot{m}_6ex_6 + \dot{m}_{26}ex_{26} = \dot{m}_1ex_1 + \dot{m}_{29}ex_{29} + \dot{Q}_{abs1}\left(1 - \frac{T_0}{T_1}\right) + \dot{E}x_{d,abs1}$
Absorber 2	$\dot{m}_{29}h_{29} + \dot{m}_{21}h_{21} = \dot{m}_{16}h_{16} + \dot{Q}_{abs2}$	$\dot{m}_{29}ex_{29} + \dot{m}_{21}ex_{21} = \dot{m}_{16}ex_{16} + \dot{Q}_{abs2}\left(1 - \frac{T_0}{T_{16}}\right) + \dot{E}x_{d,abs2}$
SHX 1	$\dot{m}_2h_2 + \dot{m}_4h_4 = \dot{m}_3h_3 + \dot{m}_5h_5$	$\dot{m}_2ex_2 + \dot{m}_4ex_4 = \dot{m}_3ex_3 + \dot{m}_5ex_5 + \dot{E}x_{d,SHX1}$
SHX 2	$\dot{m}_{17}h_{17} + \dot{m}_{19}h_{19} = \dot{m}_{18}h_{18} + \dot{m}_{20}h_{20}$	$\dot{m}_{17}ex_{17} + \dot{m}_{19}ex_{19} = \dot{m}_{18}ex_{18} + \dot{m}_{20}ex_{20} + \dot{E}x_{d,SHX2}$
RHX	$\dot{m}_{10}h_{10} + \dot{m}_{13}h_{13} = \dot{m}_{11}h_{11} + \dot{m}_{14}h_{14}$	$\dot{m}_{10}ex_{10} + \dot{m}_{13}ex_{13} = \dot{m}_{11}ex_{11} + \dot{m}_{14}ex_{14} + \dot{E}x_{d,RHX}$

PTC Analysis

In PTC analysis, the most essential parameter is its thermal efficiency, as it significantly depends upon the solar irradiation falling on the PTC arrays. The subsequent equations are applied to assess PTC. The thermal efficiency of the PTC is expressed as follows:

$$\eta_{th,PTC} = 0.75K(\theta) - 0.000045(T_{33} - T_0) - 0.039\left(\frac{T_{33}-T_0}{G}\right) - 0.3\left(\frac{T_{33}-T_0}{G}\right)^2 \quad (4.1)$$

where G is the solar irradiation and T_0 is the environment temperature (4.2)

The mass of oil (kg/s) flowing in PTC arrays is evaluated as [69]

$$\dot{m}_{oil} = 0.02A_{PTC} \quad (4.3)$$

where A_{PTC} is the total area of the PTC arrays in m^2.

Freezing Process

To evaluate the freezing process, various equations have been invoked [70]. The mass flow rate of ice formed is calculated as

$$\dot{m}_{ice} = \dot{m}_{sw}R \quad (4.4)$$

where $\dot{m}_{sw}$ is inlet seawater flow rate.

The ice ratio (R) is calculated as follows:

$$R = \frac{X_f(1-CR)}{X_d - CRX_f} \tag{4.5}$$

where *CR* is the concentration ratio, X_f is the salinity of feed water and X_d is the salinity of distill water.

The concentration ratio (*CR*) is given as $CR = \frac{X_b}{X_f}$.

The salinity of feedwater, X_f (ppm) is calculated as

$$X_f = S \times 10^6 \tag{4.6}$$

The salinity of brine (X_b) can be evaluated as

$$X_f = \frac{X_f \dot{m}_{sw} - \dot{m}_{ice} X_d}{\dot{m}_b} \tag{4.7}$$

Brine flow rate may be seen as

$$\dot{m}_b = \dot{m}_{sw}(1 - R) \tag{4.8}$$

The freezing point of the seawater, T_{freeze} (°C) can be found as [70]

$$T_{freeze} = -0.5369S - 0.0172 \qquad for\ 0.5\% \leq S \leq 4\% \tag{4.9}$$

Overall System

Overall system performance is calculated via exergy and energy efficiencies. Following expression shows the systems' energy efficiency (Figure 4.1):

$$\eta_{en,ov} = \frac{(\dot{Q}_{cooling} + \dot{E}n_{out,water} - \dot{E}n_{in,sw} + \dot{W}_{net})}{\dot{Q}_{sol}} \tag{4.10}$$

where $\dot{E}n_{out,water}$ is energy flow rate of the freshwater produced and brine, $\dot{E}n_{in,sw}$ is the energy flow rate of the input seawater. $\dot{W}_{net}$ represents the net work generated.

Following expression computes exergy efficiency of the overall setup

$$\eta_{ex,ov} = \frac{(\dot{E}x^Q_{cooling} + \dot{E}x_{out,water} - \dot{E}x_{in,sw} + \dot{W}_{net})}{\dot{E}x^Q_{sol}} \tag{4.11}$$

where $\dot{E}x^Q_{cooling} = \dot{Q}_{cooling}\left(\frac{T_0}{Tevap} - 1\right)$ and $\dot{E}x^Q_{sol} = \dot{Q}_{sol}\left[1 - \frac{4}{3}\left(\frac{T_0+273}{T_{Sun}+273}\right) + \frac{1}{3}\left(\frac{T_0+273}{T_{Sun}+273}\right)^2\right]$

4.3 Results and Discussion

Destruction rates of the exergy for the selected items in the presented setup are calculated and depicted in Figure 4.2. PTC exhibits maximum exergy destruction rate among all components (65.2% of the total exergy input), the next highest in HRVG (6.6% of the total exergy input), and third highest revealed in the condenser-2 (4.0% of the total exergy input). The highest exergy destruction in the PTC can be explained by the fact that the temperature difference across heat transfer fluid and environment is very high leading to higher generation of entropy causing higher exergy destruction. For better outcome of the overall system, attempts are thus required to decrease the exergy destruction rates in these components. These efforts need to be cost effective.

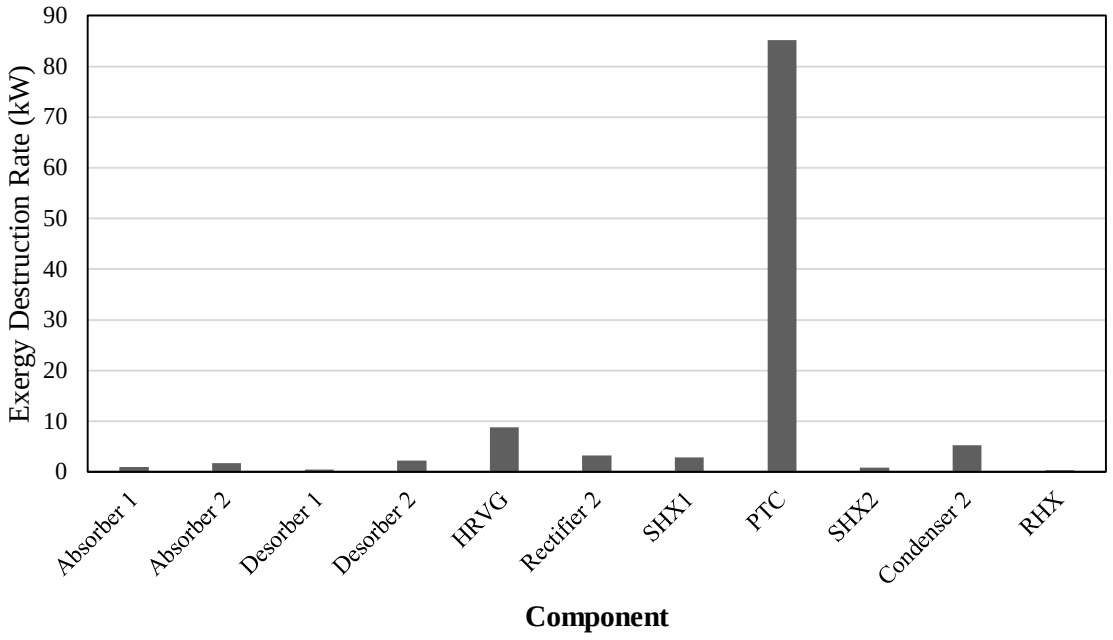

Figure 4.2 Exergy destruction rates of different element of the system

Table 4.2 provides the value of various parameter obtained for the presented system after applying the thermodynamic principles. The total work rate obtained is 3.3 kW, and the cooling rate produced by the system is 20.4 kW. The exergy efficiency of PTC field is found to be

29.8%, while its energy efficieny as 70.0% for solar irradiation of 700 W/m^2. These results match closely with the value found by Bellos et al. [71]. Analysis also reveals that an area of 200 m^2 of PTC is required to produce 0.01 kg/s of freshwater (see Table 4.2).

Table 4.2 Input and calculated parameter values from feasibility analysis

Parameter	**Value**
Net Work rate of the system (kW)	3.3
Rate of cooling (kW)	20.4
Systems' exergy efficiency (%)	4.7
Systems' energy efficiency (%)	18.8
Evaporator Temperature (℃)	-10
Solar irradiation (kW/m^2)	0.7
Ambient Temperature (℃)	25
Sun Temperature (℃)	5497
$K(\theta)$	1
Area of PTC arrays (m^2)	200
Rate of freshwater produced (kg/s)	0.01
Salinity, S (%)	0.5
Ice ratio, R	0.4
Freezing temperature (℃)	-0.29
Seawater inlet temperature (℃)	25
Energy efficiency of PTC (%)	70.0
Exergy efficiency of PTC (%)	29.8

Efficiencies of the overall setup are evaluated by varying the solar irradiation (DNI) in Figure 4.3. It is seen that system performs efficiently at higher solar irradiance (DNI). Energy efficiency of the overall setup varies from 11.2% to 24.2% with the variation of solar irradiance from 500 W/m^2 at 1000 W/m^2 which is about 120% increase in given range of solar irradiance. Similarly, systems' exergy efficiency varies from 4.4% to 4.8% with similar variation of solar irradiance which is about 9.0% increase in given range of solar irradiance. This happens because the rise in

solar energy input, refrigeration effect of vapor absorption system rises, resulting in the increase in cooling output of the cycle eventually causing efficiencies of the overall setup to enhance.

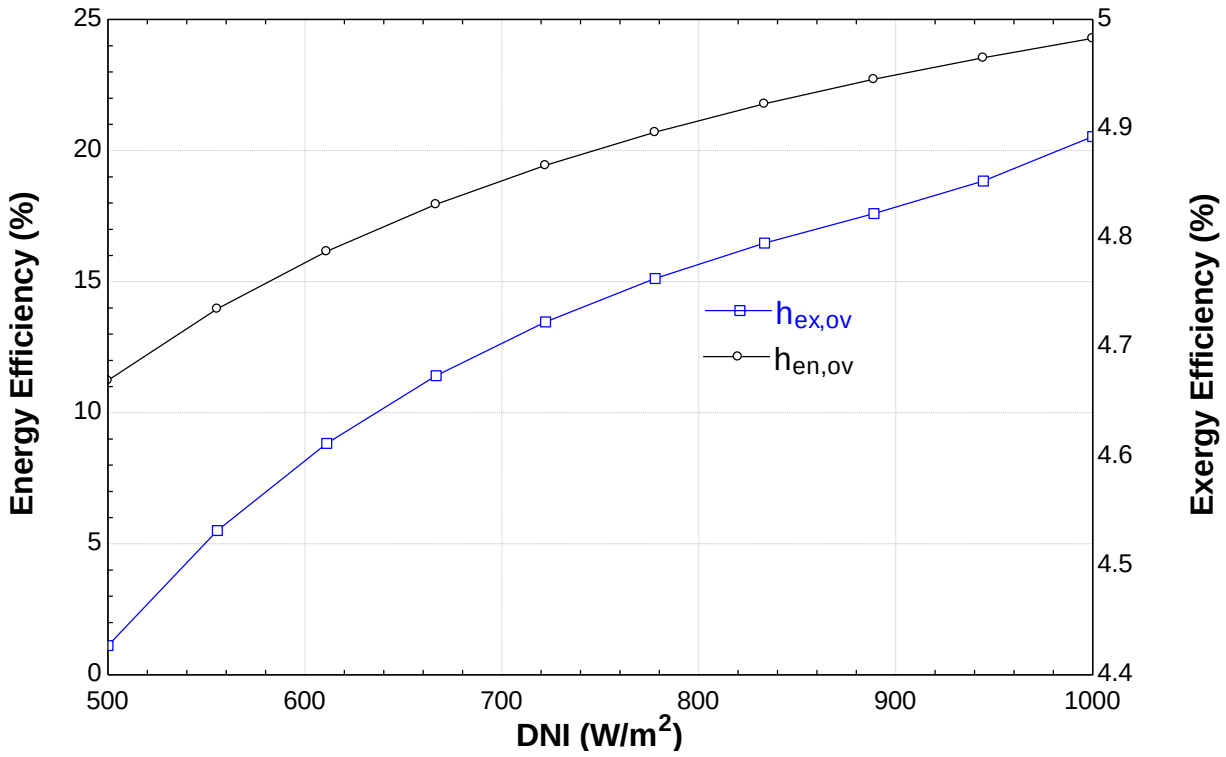

Figure 4.3 Variation of systems' exergy and energy efficiencies with the solar irradiance (DNI)

Figure 4.4 depicts the variation of both efficiencies of the overall setup by rising in evaporator temperature (T_{13}) of the vapor absorption system. The systems' energy efficiency enhanced from 18.8% to 23.0% with change in evaporator temperature from -10℃ to -5℃. The exergy efficiency of the setup varies slightly (4.7% - 4.9%). Increasing the evaporator temperature, the cooling effect rises causing systems' energy efficiency to rise. As the evaporator temperature increases, the magnitude of Carnot factor $(1 - \frac{T_0}{Tevap})$ decreases. However, the rate at which Carnot factor decreases is less compared to the rate at which cooling effect increases, which lead to enhancement of exergy efficiency of the overall system.

Figure 4.5 highlights the dependence of performance of the overall setup and freezing temperature with the rise in salinity (S). The systems' exergy and energy efficiencies decline marginally with the rise in salinity. As the salinity varies, the freezing temperature drops which

means more cooling effect is required to freeze the seawater and consequently results in lowering of both the efficiencies in overall setup.

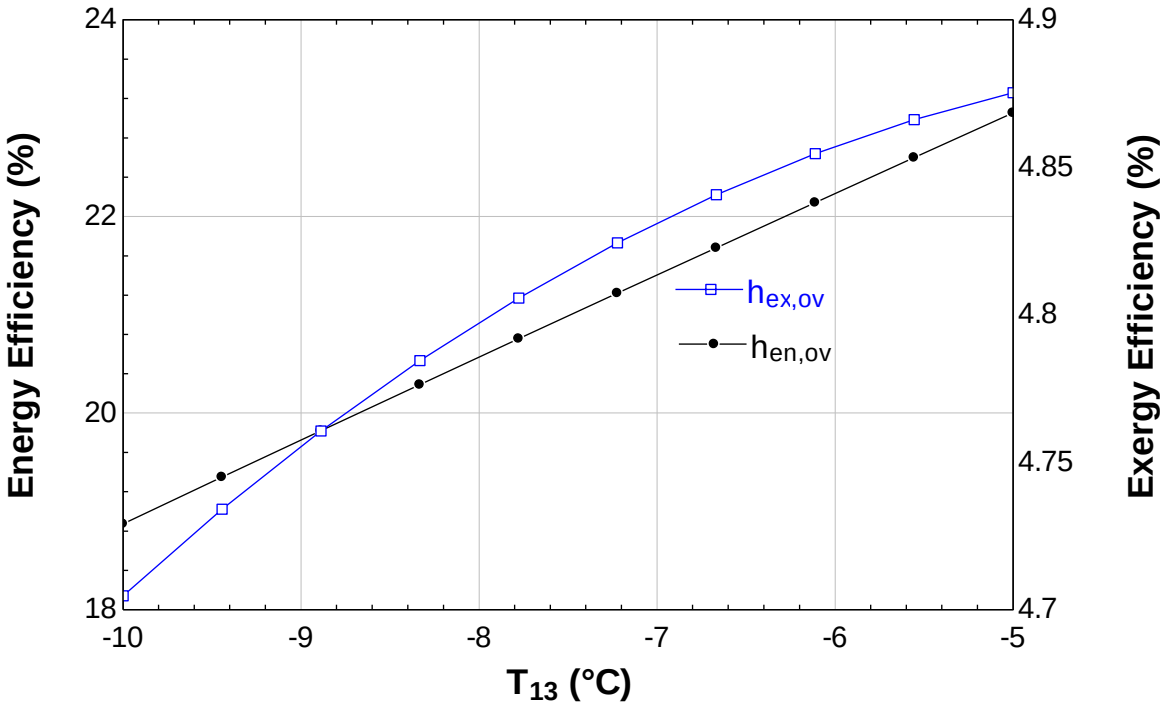

Figure 4.4 Result of evaporator temperature (T_{13}) on systems' exergy and energy efficiencies

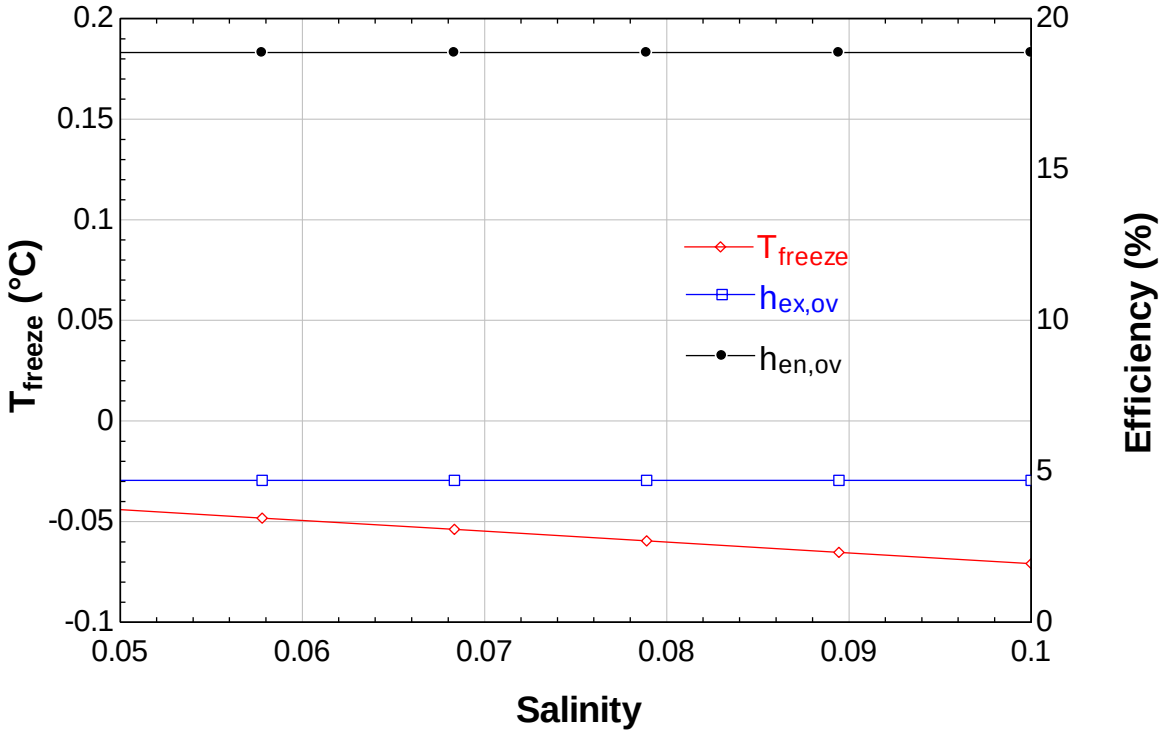

Figure 4.5 Results of systems' exergy and energy efficiencies and freezing temperature (T_{freeze}) with the seawater salinity (S)

Figure 4.6 shows the changes of systems' exergy and energy efficiencies with the change in seawater inlet temperature (T_{sw}). As the seawater inlet temperature ranges from 28℃ to 40℃, the systems' energy efficiency alters very slightly i.e. 18.8% to 19.1%. However, the exergy efficiency of the overall setup varies 4.9% to 5.5%. This trend is mainly observed because with the rise in seawater inlet temperature, the exergy content of cooling and freshwater both increases results in the enhanced exergy efficiency of the setup.

Fluctuations in both efficiencies of the overall setup with the increment of the mass flow rate of freshwater produced is illustrated (Figure 4.7). Change in mass flow rate of freshwater from 0.005 to 0.02 kg/s, the energy efficiency of the setup varies very significantly i.e. 20.0% to 16.4%. Though, the exergy efficiency of the setup alters from 4.9% to 4.1%. This trend is mainly observed because with the rise in the flow rate of freshwater produced, rate of cooling required to freeze the water increases and the cooling output obtained by the system decreases causing the reduction in both the systems' efficiencies.

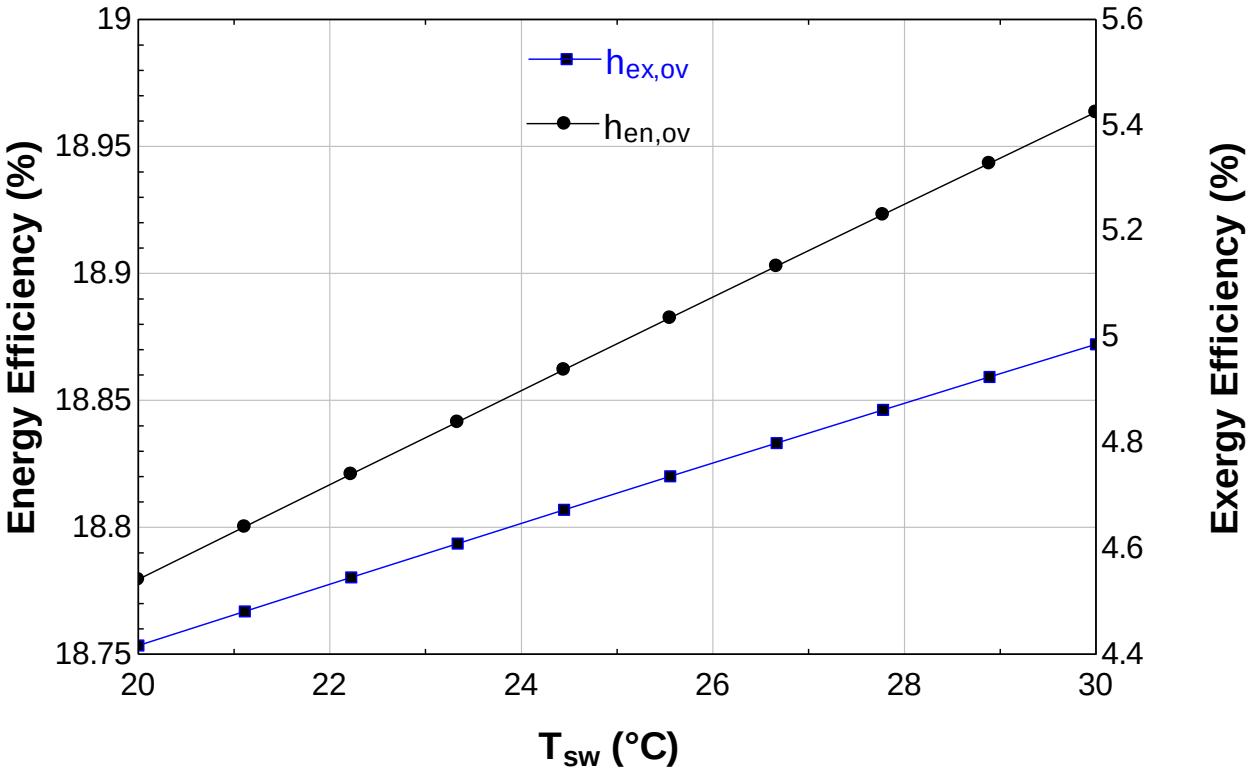

Figure 4.6 Variation of systems' exergy and energy efficiencies with the seawater inlet temperature (T_{sw})

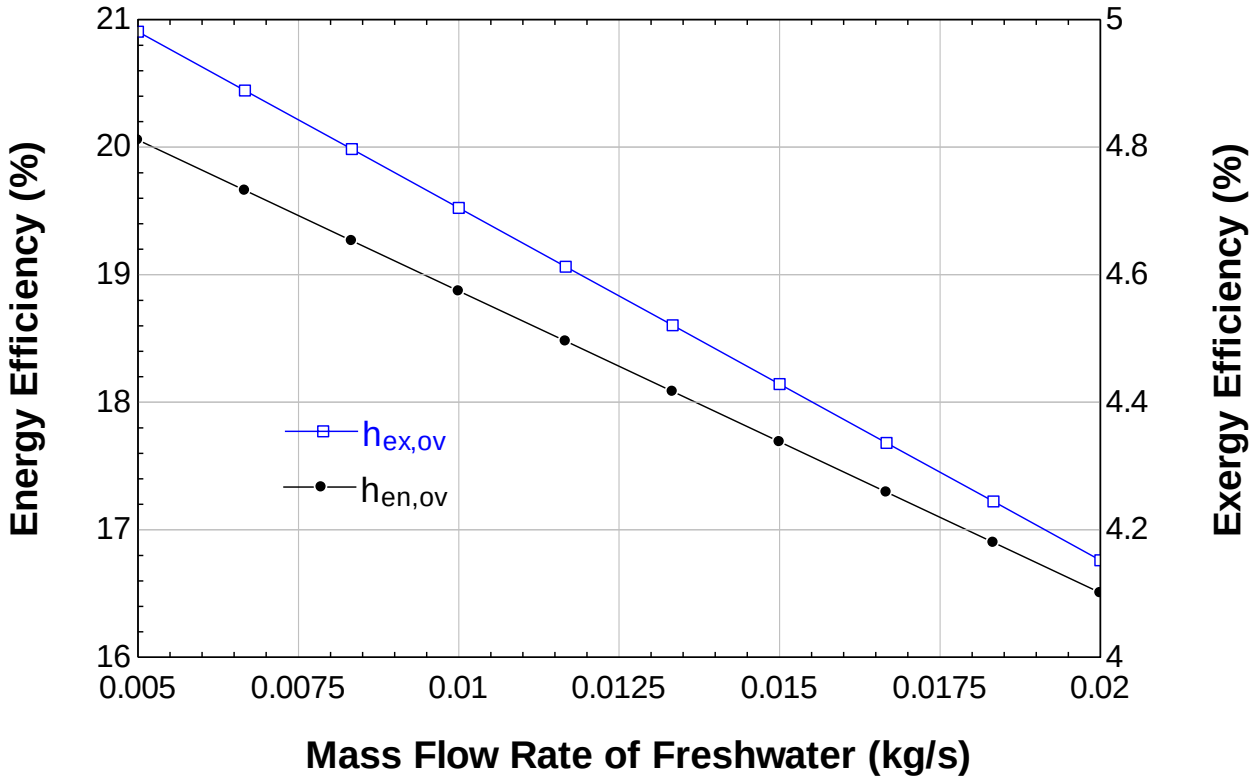

Figure 4.7 Effect of freshwater produced on the systems' exergy and energy efficiencies

Figure 4.8 shows the variation of ice ratio of the overall system with the freshwater produced. As the ice ratio changes, the energy consumed for freezing decreases and cooling obtained by the system ($\dot{Q}_{cooling}$) increases which causes the systems' energy efficiency to be almost constant. The systems' exergy efficiency changes from 4.1% to 4.7%. This trend is mainly observed because with the increase in the ice ratio, amount of exergetic cooling required to freeze the water decreases and the exergetic cooling output ($\dot{E}x^{Q}_{cooling}$) obtained by the system increases. However, the rate at which the exergetic cooling output obtained by the system increases supersede the rate at which the amount of the exergetic cooling required to freeze the water reduces causing the exergy efficiency enhancement in the overall system.

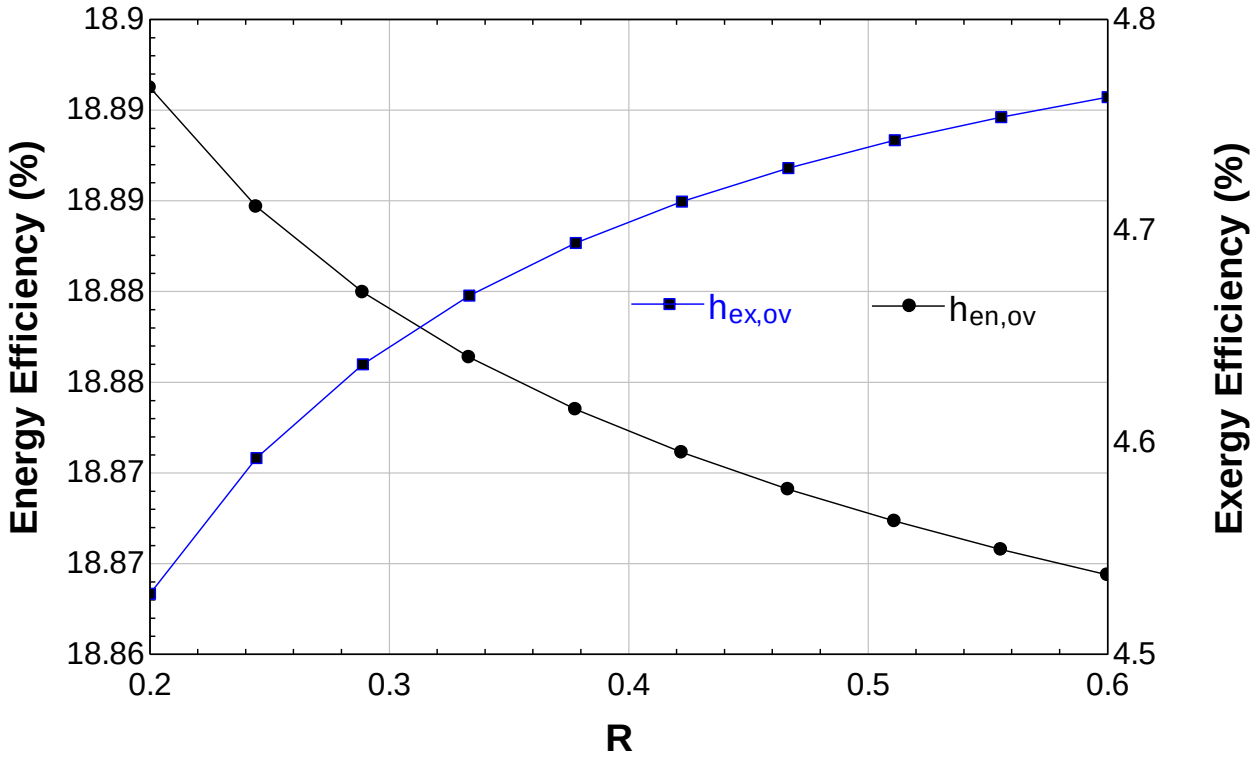

Figure 4.8 Variation of systems' energy and exergy efficiencies with the ice ratio (R)

Chapter 5

Conclusions and Recommendations for Future Work

5.1 Conclusions

This thesis presented three solar energy based polygeneration systems (one may call them as System 1, System 2, and System 3) for catering the demand (electricity, hydrogen, cooling etc.) of a self sustained community. The presented systems are examined via energy and exergy analyses for better solar energy utilization. The conclusions made from the analysis presented in chapters (namely Chapter 2, Chapter 3 and Chapter 4) are presented as below:

For System 1 (presented in Chapter 2), the conclusions are as follows:

- With the change in solar irradiance from 400 W/m^2 to 1000 W/m^2, systems' overall energy efficiency changes from 36.6% to 40.2%, while systems' exergy efficiency rises from 16.6% to 18.6%, and the net work rate increases from to 195.8 kW to 558.7 kW while cooling capacity rises from 338 kW to 873 kW. The rate of hydrogen generated also rises with the rise in solar irradiance i.e., 0.0019 kg/s to 0.003 kg/s.
- The designed system provides the electricity of around 372 kW which will cater the electric power in an environmentally benign manner on an average sunny day of 6 hrs with an average DNI of 700 W/m^2. Additionally, it can provide a cooling capacity of 3 kW to each house. The produced hydrogen can fuel 100 vehicles with an average range of 100 km per day.
- So, System 1 will be suitable for the location where sufficient sunshine is available to produce hydrogen, electricity and cooling for a residential community of 200 houses (800 people).

For System 2 (presented in Chapter 3), the conclusions are as follows:

- Thermodynamic assessment of the parabolic trough based polygeneration system shows that with the change in irradiation changes from 300 W/m^2 to 1000 W/m^2, the energy and exergy efficiencies of the overall system changes from 14.6% to 17.8%, and 9.1% to 11.1%, respectively. As the direct normal irradiation rises, the rate of hydrogen production increases from 0.00015 kg/s to 0.00062 kg/s, electrical work increases from 25.9 kW to 105 kW , rate of freshwater changes from 6.6 kg/d to 27.0 kg/d, and cooling rate changes from 40.0 kW to 163 kW.
- Results show that the demand for electricity, hydrogen etc can be met with the designed system in a more efficient and benign way. Thus, System 2 can be installed or recommended for the location having sufficient sunshine and scarcity of potable drinking

water. The designed system produced four useful outputs namely, electricity, cooling, freshwater and hydrogen for the community of 250 people.

For System 3 (presented in Chapter 4), the conclusions are as follows:

- Simulation results show that the systems' energy efficiency is 18.8% and the systems' exergy efficiency is 4.7%.
- Energy efficiency of the overall setup varies from 11.2% to 24.2% with the variation of solar irradiance from 500 W/m^2 at 1000 W/m^2 which is about 120% increase in given range of solar irradiance. Similarly, systems' exergy efficiency varies from 4.4% to 4.8% with similar variation of solar irradiance which is about 9.0% increase in given range of solar irradiance.
- While System 3 can be implemented in the location where there is a need of cooling, electricity and freshwater with an abundance of sunshine and source of saline water. The result presented in the current thesis may help the designers/researcher to create a self-sustained community in a more environmental and benign manner.

The overall conclusions are as follows:

- System 1 has higher efficiency compared to System 2 and 3. This is mainly due to high operating temperature originating from the heliostat field system. However, the system requires larger area and have materialistic disadvantages.
- Although System 2 has inferior efficiency than System 1 but it offers advantages like lesser solar area and low operating temperature leading to less operational challenges.
- Depending upon the available area and operating temperature of the solar system, the design engineer could choose either System 1 or System 2 for meeting various energy demands. The only difference is being in the useful output produced which is freshwater.
- System 3 has the least exergy efficiency among all systems. Systems 1 and 2 has hydrogen as the useful output which can acts an energy vector during the off peak hours for meeting out the energy demand. However, System 3 does not have hydrogen as an useful output which makes brings the exergy efficiency of the system less than 200% to 400% compared to former systems. This clearly shows the benefit of hydrogen production as an useful output in any solar energy conversion process. However, system

3 can be used in place of VCR based freezing desalination processes as it offers better efficiency compared to them.

5.2 Recommendations for Future Work

The proposed systems provide a potential option for solar dominated remote areas to obtain cooling, freshwater, hydrogen and electrical power in an environmentally safer manner. The result presented in the current thesis may help the designers/researcher to create the self sustained community in a more environmental and benign manner. Following recommendation for future work can be made based on the results obtained in the current study:

- Economic Analysis of the presented systems should be done for better cost effectiveness
- Life cycle assessment of the presented systems should be done for overall environmental impact
- Other hydrogen production technologies, such as thermochemical cycles etc. should be investigated
- The prototype of the presented systems should be developed

References

[1] World Energy Outlook, International Energy Agency, 2021 (accessed on 9 July 2021). https://www.iea.org/data-and-statistics/data-browser/?country=WORLD&fuel=CO2%20emissions&indicator=CO2BySource

[2] Cohce, M. K., I. Dincer and M. A. Rosen (2011). Energy and exergy analyses of a biomass-based hydrogen production system, Bioresource Technology 102(18), 8466-8474.

[3] Khalid, F., I. Dincer and M. A. Rosen (2015). Energy and exergy analyses of a solar biomass intergated cycle for multigeneration, Solar energy 112, 290-299.

[4] Demir, M.E. and I. Dincer (2018). Development and analysis of a new integrated solar energy system with thermal storage for fresh water and power production, International Journal of Energy Research 42 (9), 2864-2874.

[5] Sakthivadivel, D., K. Balaji, D. Dsilva Winfred Rufuss, S. Iniyan and L. Suganth (2021). Renewable-Energy-Driven Future: Technologies, Applications, Sustainability, and Policies, J Ren, Ed., Elsevier, pp: 1-42.

[6] Borunda, M., O.A. Jaramillo, R. Dorantes and A. Reyes (2016). Organic Rankine Cycle coupling with a Parabolic Trough Solar Power Plant for cogeneration and industrial processes, Renewable Energy 86, 651-663.

[7] Dincer, I and C. Zamfirescu (2012). Renewable-energy-based multigeneration systems, International Journal of Energy Research 36, 1403–1415.

[8] Al-Sulaiman, F.A., F. Hamdullahpur and I. Dincer (2011). Performance Comparison of Three Trigeneration Systems Using Organic Rankine Cycles, Energy 36, 5741-5754.

[9] Malico, I., A.P. Carvalhinho and J. Tenreiro. (2009). Design of a trigeneration system using a high-temperature fuel cell, International Journal of Energy Research 33, 144-51.

[10] Khalid, F., I. Dincer and M. A. Rosen (2017). Thermoeconomic analysis of a solar-biomass integrated multigeneration system for a community, Applied Thermal Engineering 120, 645-653.

[11] Dagdougui, H., R. Minciardi, A. Ouammi, M. Robba and R. Sacile (2012). Modeling and optimization of a hybrid System for the energy supply of a “Green” building. Energy Conversion and Management 64, 351-363.

[12] Mitali, J., Dhinakaran, S., and A.A. Mohamad (2022). Energy storage systems: a review, Energy Storage and Saving 1, 166–216.

[13] L. Al-Ghussain, R. Samu, O. Taylan and M. Fahrioglu (2020). Sizing renewable energy systems with energy storage systems in microgrids for maximum cost-efficient utilization of renewable energy resources. Sustainable Cities and Society 55, 102059.

[14] Chakraborty, M.R., Dawn, S., Saha, P.K., Basu, J.B. and Ustun, T.S (2022). A Comparative Review on Energy Storage Systems and Their Application in Deregulated Systems, Batteries 8, 124.

[15] Hadjipaschalis, I., A. Poullikkas and V. Efthimiou (2009). Overview of current and future energy storage technologies for electric power applications. Renewable and Sustainable Energy Reviews 13: 1513–1522.

[16] Dincer, I (2007). Environmental and sustainability aspects of hydrogen and fuel cell systems, International Journal of Energy Research 31, 29-55.

[17] Lokar, J., and Virtic, P (2020). The potential for integration of hydrogen for complete energy self-sufficiency in residential buildings with photovoltaic and battery storage systems, International Journal of Hydrogen Energy 45, 34566-34578

[18] Harnessing Green Hydrogen: Opportunities for Deep Decarbonisation in India, NITI Aayog (2022), RMI, https://www.niti.gov.in/documents/reports/ (accessed on 29 July 2022).

[19] Song, H., Luo, S., Huang, H., Deng, B., and Ye, J (2022). Solar-Driven Hydrogen Production: Recent Advances, Challenges, and Future Perspectives, ACS Energy Letter 7, 1043–1065.

[20] Wang et al. (2023). Potential technology for seawater electrolysis: Anion-exchange membrane water electrolysis, Chem Catalysis 3, 100643.

[21] Khalid, F., I. Dincer and M.A. Rosen (2016). Comparative assessment of CANDU 6 and Sodium-cooled Fast Reactors for nuclear desalination, Desalination 379, 182-192.

[22] Khalid, F., I. Dincer and M.A. Rosen (2016). "Analysis and Assessment of a Gas Turbine-Modular Helium Reactor for Nuclear Desalination", ASME Journal of Nuclear Engineering and Radiation Science, 2(3), 031014.

[23] Sahin, S., H.M. Sahin, T.A. Kusayer, F. Sefidvash (2011). "An innovative nuclear reactor for electricity and desalination", International Journal of Energy Research 35, 96-102.

[24] Kim, H.S. and H.C. No (2014). "Thermal coupling of HTGRs and MED desalination plants, and its performance and cost analysis for nuclear desalination", Desalination 303,17-22.

[25] Youssef, P., R. Al-Dadah and S. Mahmoud (2014). "Comparative analysis of desalination technologies", Energy Procedia 61, 2604-2607.

[26] Brandt, M. J., et al. The IDA Water Security Handbook 20192020, Water desalination report https://www.desalination.com/publications/catalogue/ida-handbook .

[27] Al-Karaghouli A, Kazmerski LL. Energy consumption and water production cost of conventional and renewable-energy-powered desalination processes. Renew Sustain Energy Rev 2013;24:34356.

[28] Mehmood, A, and Jingzheng Ren (2021). Renewable-Energy-Driven Future: Technologies, Applications, Sustainability, and Policies, J Ren, Ed., Elsevier, pp: 333-374.

[29] Attia, A.A.A (2010). "New proposed system for freeze water desalination using auto reversed R-22 vapor compression heat pump" Desalination 254, 179-184

[30] Meng, X., Yang, F., Bao, Z., Deng, J., Serge, N.N., and Zhang, Z (2010). Theoretical study of a novel solar trigeneration system based on metal hydrides, Applied Energy 87, 2050–61.

[31] Ghasemi, A., Heidarnejad, P. and Noorpoor, A (2018). A novel solar-biomass based multi-generation energy system including water desalination and liquefaction of natural gas system: Thermodynamic and thermoeconomic optimization, Journal of Cleaner Production 196, 424–47.

[32] Rokni, M (2019). Analysis of a polygeneration plant based on solar energy, dual mode solid oxide cells and desalination, International Journal of Hydrogen Energy 44, 19224–43.

[33] Bai, Z., Liu, Q., Lei, J., Li, H., and Jin, H (2015). A polygeneration system for the methanol production and the power generation with the solar–biomass thermal gasification, Energy Conversion and Management 102, 190–201.

[34] Yu, H., H. Helland, X. Yu, T. Gundersen and G. Sin (2021). "Optimal design and operation of an Organic Rankine Cycle (ORC) system driven by solar energy with sensible thermal energy storage", Energy Conversion and Management 244, 114494.

[35] Quoilin, S., M. Orosz, H. Hemond and V. Lemort (2011). "Performance and design optimization of a low-cost solar organic Rankine cycle for remote power generation", Solar Energy 85, 955-966.

[36] Fernández-Guillamón, A., A. Molina-García, F. Vera-García and J.A. lmendros-Ibáñez (2021). "Organic Rankine Cycle Optimization Performance Analysis Based on Super-Heater Pressure: Comparison of Working Fluids" Energies 14, 2548.

[37] Tchanche, B.F., G. Papadakis, G. Lambrinos and A. Frangoudakis (2009). "Fluid selection for a low-temperature solar organic Rankine cycle", Applied Thermal Engineering 2009, 2468-2476.

[38] Al-Sulaiman, F. A., F. Hamdullahpur and I. Dincer (2012). "Performance assessment of a novel system using parabolic trough solar collectors for combined cooling, heating, and power production", Renewable Energy 48, 161-172.

[39] Al-Sulaiman, F.A (2014). "Exergy analysis of parabolic trough solar collectors integrated with combined steam and organic Rankine cycles", Energy Conversion and Management 77, 441-449.

[40] Pourmoghadam, P. and A. Kasaeian (2023) "Economic and energy evaluation of a solar multi-generation system powered by the parabolic trough collectors", Energy 262, 125362.

[41] Khalid, F., R. Kumar and F. Khalid (2021). “Feasibility study of a new solar based trigeneration system for fresh water, cooling, and electricity production” International Journal of Energy Research 45 (13), 19500-19508.

[42] Xu, C., Z.Wang, X. Li and F. Sun (2011) “Energy and exergy analysis of solar power plants” Applied Thermal Engineering 31, 3904-3913.

[43] Pelay, U., L. Luo, Y. Fan, D. Stitou and C. Castelain (2019). “Integration of a thermochemical energy storage system in a Rankine cycle driven by concentrating solar power: Energy and exergy analyses” Energy 167, 498-510.

[44] Jaubert, H., P. Borel, P. Guichardon, J. Portha, J. Jaubert and L. Coniglio (2021). “Assessment of organic Rankine cycle configurations for solar polygeneration orientated to electricity production and desalination” Applied Thermal Engineering 195,116983.

[45] Hamilton, W.T., A. M. Newman, M. J.Wagner and R. J. Braun (2020) “Off-design performance of molten salt-driven Rankine cycles and its impact on the optimal dispatch of concentrating solar power systems” Energy Conversion and Management 220, 113025.

[46] Azzam, A and I. Dincer (2021). “Development and analysis of an integrated solar energy system for smart cities” Sustainable Energy Technologies and Assessment 46, 101170.

[47] Tukenmez, N., M. Koc and M. Ozturk (2021). “A novel combined biomass and solar energy conversion-based multigeneration system with hydrogen and ammonia generation” International Journal of Hydrogen Energy 46, 16319-16343.

[48] Rovense, F., M. A. Reyes-Belmonte, M. Romero, J. Gonzalez-Aguilar (2022). “Thermo-economic analysis of a particle-based multi-tower solar power plant using unfired combined cycle for evening peak power generation” Energy 240, 22798.

[49] Kahraman, U and I. Dincer (2022). “Performance analysis of a solar based waste to energy multigeneration system” Sustainable Energy Technologies and Assessments 50, 101729.

[50] Alirahmi, S.M., A. Khoshnevisan, P. Shirazi, P. Ahmadi and D. Kari (2022). “Soft computing based optimization of a novel solar heliostat integrated energy system using artificial neural networks” Sustainable Energy Technologies and Assessment 50, 101850.

[51] Yimaz, F., M. Ozturk, and R. Selbas (2023). “Development and assessment of a solar-driven multigeneration plant with compressed hydrogen storage for multiple useful products”, International Journal of Hydrogen Energy (in press).

[52] Bozgeyik, A., L. Altay and A. Hepbasli (2022). “A parametric study of a renewable energy based multigeneration system using PEM for hydrogen production with and without once-through MSF desalination”, International Journal of Hydrogen Energy 47, 31742-31754.

[53] Yuksel, Y.E., M.Ozturk and I. Dincer (2022). “Design and analysis of a new solar hydrogen plant for power, methane, ammonia and urea generation”, International Journal of Hydrogen Energy 47, 19422-1 944 5.

[54] Derbal-Mokrane, H., F. Amrouche, M.N. Omari and I. Yahmi (2021). “Hydrogen production through parabolic trough power plant based on the Organic Rankine Cycle implemented in the Algerian Sahara”, International Journal of Hydrogen Energy 46, 32768-32782.

[55] Yimaz, F., M. Ozturk, and R. Selbas (2022). “Investigation of the thermodynamic analysis of solar Energy-based multigeneration plant for sustainable multigeneration”, Sustainable Energy Technolgies and Assessment 53, 102461.

[56] Toghyani, S., E. Afshari, E. Baniasadi and M.S. Shadloo (2019). Energy and exergy analyses of a nanofluid based solar cooling and hydrogen production combined system”, Renewable Energy 141, 1013-1025.

[57] Yuksel, Y.E (2018). “Thermodynamic assessment of modified Organic Rankine Cycle integrated with parabolic trough collector for hydrogen production” International Journal of Hydrogen Energy 43, 5832-5841.

[58] Abdelhay, A., Fath, H.S., and Nada, S.A (2020). Solar driven polygeneration system for power, desalination and cooling, Energy 198, 117341.

[59] Calise, F., Dentice d'Accadia, M., Vanoli, R., and Vicidomini, M (2019). Transient analysis of solar polygeneration systems including seawater desalination: A comparison between linear Fresnel and evacuated solar collectors, Energy 172, 647–660.

[60] Ghorbani, B., Miansari, M., Zendehboudi, S., and Hamedi, M.H (2020). Exergetic and economic evaluation of carbon dioxide liquefaction process in a hybridized system of water desalination, power generation, and liquefied natural gas regasification, Energy Conversion and Management 205, 112374.

[61] Vazini, M.H. and Manesh, M.H.K (2021). 4E dynamic analysis of a water-power cogeneration plant integrated with solar parabolic trough collector and absorption chiller, Thermal Science and Engineering Progress 21, 100785.

[62] Keshavarzzadeh, A.H., Ahmadi, P., and Rosen, M.A (2020). Technoeconomic and environmental optimization of a solar tower integrated energy system for freshwater production, Journal of Cleaner Production 270, 121760.

[63] Esmaeilion, F.,Soltani, M., and Nathwani, J (2022). Assessment of a novel solar-powered polygeneration system highlighting efficiency, exergy, economic and environmental factors, Desalination 540, 116004.

[64] Serra, L.M., Lozano, M.A, Ramos, J, Ensinas, A.V, and Nebra, S.A (2009) "Polygeneration and efficient use of natural resources" Energy 34, 575–586.

[65] El-Emam, R. and I. Dincer (2018). "Development and assessment of a novel solar heliostat-based multigeneration system" International Journal of Hydrogen Energy 43, 2610-2620.

[66] Xu, F., D.Y. Goswami and S.S. Bhagwat (2000) "A Combined Power/Cooling" Energy 25, 233-246.

[67] Xu, C., Z.Wang, X. Li and F. Sun (2011) "Energy and exergy analysis of solar power plants" Applied Thermal Engineering 31, 3904-3913.

[68] Hu, Y., Z. Xu, C. Zhou, J. Du and Y. Yao (2020). "Design and performance analysis of a multi-reflection heliostat field in solar power tower system" Renewable Energy 160, 498-512.

[69] Tzivanidis, C., E. Bellos, K. A. Antonopoulos (2016). “Energetic and financial investigation of a stand-alone solar-thermal Organic Rankine Cycle power plant”, Energy Conversion and Management 126, 421-433.

[70] Abd Elrahman, M.A., S. Abdo, E. Hussein., A. A. Altohamy and A. A. A. Attia (2019). “Exergy and parametric analysis of freeze desalination with reversed vapor compression cycle”, Thermal Science and Engineering Progress 19, 100583.

[71] Bellos, E., C. Tzivanidis and K. A. Antonopoulos (2016). “Exergetic and energetic comparison of LiCl-H2O and LiBr-H2O working pairs in a solar absorption cooling system”, Energy Conversion and Management 123, 453-461.